nature communications

Article

https://doi.org/10.1038/s41467-025-60073-0

Enhancing the potency of in vivo lentiviral vector mediated gene therapy to hepatocytes

Received: 1 July 2024

Accepted: 12 May 2025

Published online: 23 May 2025

Check for updates

Cesare Canepari[1,2], Michela Milani[1], Chiara Simoni[1,2], Francesco Starinieri[1,2], Monica Volpin[1], Anna Fabiano[1], Mauro Biffi[1], Fabio Russo[1], Rossana Norata[1], Martina Rocchi[3], Chiara Brombin[4], Federica Cugnata[4], Eugenio Montini[1], Francesca Sanvito[3], Markus Grompe[5] & Alessio Cantore[1,2]

In vivo gene therapy to the liver using lentiviral vectors (LV) may represent a one-and-done therapeutic approach for monogenic diseases. Increasing LV gene therapy potency is crucial for reducing the effective doses, thus alleviating dose-dependent toxicities and facilitating manufacturing. LV-mediated liver transduction may be enhanced by positively selecting LV-transduced hepatocytes after treatment (*a posteriori*) or by augmenting the initial fraction of LV-targeted hepatocytes (a priori). We show here that the *a posteriori* enhancement increased transgene output without expansion of hepatocytes bearing LV genomic integrations near cancer genes, in mouse models of hemophilia, an inherited coagulation disorder. Furthermore, we enhanced hepatocyte transduction a priori in mice by transiently inhibiting antiviral pathways and/or through a fasting regimen. The most promising transduction-enhancer combination synergized with phagocytosis-shielded LV, resulting in a remarkable 40-fold increase in transgene output. Overall, our work highlights the potential of minimally invasive, cost-effective treatments capable of improving the potency of in vivo LV gene therapy to hepatocytes, in order to expand its applicability and ease clinical translation.

Mutations in genes expressed by hepatocytes cause a plethora of monogenic diseases, which may be treated by in vivo viral vector-based liver-directed gene addition[1]. Adeno-associated viral (AAV) vectors are at the most advanced stage of development in in vivo gene therapy. AAV vectors encoding coagulation factors have successfully been administered to adult individuals affected by hemophilia, showing multi-year clinical benefits[2,3]. These promising clinical results led to the commercial approval of AAV-vector mediated liver gene therapies for adults with hemophilia A or hemophilia B, which are due to mutations in the gene encoding for coagulation factor VIII (FVIII), or factor IX (FIX), respectively. However, AAV vector genomes are progressively diluted during hepatocyte proliferation due to their mostly episomal conformation in target cells, challenging the treatment of pediatric patients. Moreover, pre-existing immunity against AAV components is frequent in humans. This currently limits applications of in vivo AAV-vector gene therapy to individuals with low anti-AAV antibody titers and imposes transient immune suppression to maintain transduced hepatocytes, which transiently expose AAV capsid antigens[4]. In contrast, lentiviral vectors (LV) integrate into the genome of target cells and are maintained upon cell proliferation, thus

[1]San Raffaele Telethon Institute for Gene Therapy, IRCCS San Raffaele Scientific Institute, Milan, Italy. [2]Vita-Salute San Raffaele University, Milan, Italy. [3]IRCCS San Raffaele Scientific Institute, Milan, Italy. [4]Center for Statistics in the Biomedical Sciences, Vita-Salute San Raffaele University, Milan, Italy. [5]Oregon Health and Science University, Oregon, US. e-mail: cantore.alessio@hsr.it

potentially allowing for long-lasting transgene expression by a single administration, even in young individuals. Moreover, pre-existing anti-LV immunity in humans is rare. We and others previously showed stable LV-mediated liver gene transfer in both small and large animal models, resulting in the correction of hemophilia and other inherited liver diseases[5–9]. More recently, we engineered LV to bear a high surface content of the phagocytosis inhibitor CD47 (CD47hi-LV) and improved the efficiency of hepatocyte transduction in vivo[7].

To progress toward clinical testing of in vivo LV gene therapy, it would be essential to further increase the potency of gene transfer to hepatocytes. This would allow for reducing the effective LV doses, thus facilitating the manufacturing of high quantities of highly purified LV and alleviating potential LV dose-dependent toxicities and immune activation. Enhancing the potency of liver gene therapy would be useful for both non-cell autonomous diseases, such as hemophilia, and even more for cell-autonomous diseases, in which achieving the therapeutic outcome may be more challenging. Indeed, in the context of secreted transgenes, correcting a small percentage of hepatocytes may be sufficient, enforcing supraphysiological transgene expression *per* cell. Nevertheless, the production of high amounts of transgene *per* cell may be harmful to hepatocytes in some cases, as has been proposed for FVIII[10]. By contrast, cell-autonomous diseases may require a high percentage of corrected liver mass for efficacy, thus demanding higher doses or higher potency. An increase in LV potency may be achieved by positively selecting LV-transduced hepatocytes after treatment (transduction enhancement *a posteriori*) or by augmenting the initial fraction of hepatocytes transduced by LV (transduction enhancement at the time of transduction or a priori).

Concerning transduction enhancement *a posteriori*, a strategy to endow transduced hepatocytes with a selective advantage has been recently proposed[11,12]. In this strategy, the therapeutic transgene is coupled with a short hairpin RNA (shRNA) targeting NADPH-cytochrome P450 oxidoreductase (Cypor), an indispensable redox partner for all microsomal cytochrome P450 (Cyp450) enzyme activity. As a consequence, transduced hepatocytes with low Cypor activity are more resistant than untransduced ones to toxic doses of acetaminophen (paracetamol), a safe and well-known anti-inflammatory drug, with exclusively hepatic toxicity when overdosed. This toxicity is due to Cyp450 activity on a small fraction of acetaminophen, which is converted into a toxic metabolite that leads to hepatocyte necrosis[13]. Cyp450s are primarily active in hepatocytes located in the area of the liver lobule close to the central vein (also known as peri-central or zone-3 hepatocytes). Peri-central hepatocyte damage and subsequent necrosis are induced exclusively in the non-corrected hepatocytes, with normal Cypor activity. Corrected hepatocytes replace the damaged ones, with subsequent increases in transgene output over time.

Concerning transduction enhancement a priori, different pathways and drugs have been described to increase transduction efficiency by viral vectors. Firstly, proteasome inhibition has been shown to improve LV-mediated gene transfer in hematopoietic stem/progenitor cells ex vivo[14]. Proteasome activity may indeed degrade vector capsids during uncoating or factors required by the vector for efficient transduction. For this reason, transient blockage of proteasome activity may be applied to improve liver-directed LV-mediated gene therapy. Secondly, mice lacking a functional interferon (IFN) alpha and beta receptor subunit 1 (IFNAR1) display higher liver gene transfer than wild-type (WT) mice by LV[15]. A transient blockage of IFNAR1 may thus be an additional means to improve in vivo LV-mediated gene transfer to hepatocytes. Transduction enhancement has been attempted even in the context of AAV-vector gene therapy for the liver. An effective way to achieve it has been by fasting mice or non-human primates[16]. Based on these premises, we selected three possible enhancers of LV transduction of hepatocytes, specifically a proteasome inhibitor, an anti-IFNAR1 monoclonal antibody, and fasting, that may prime target cells to allow high transduction efficiency, i.e., transduction enhancement a priori.

Here, we applied the positive selection strategy to WT or hemophilic mice treated at different ages with different LV, achieving therapeutic transgene amounts starting from low LV doses, and assessed the profile of LV genomic integration sites in mice with clonally expanded hepatocytes, overall confirming and extending previous results related to this strategy. Furthermore, we report successful improvement of the potency of in vivo LV gene therapy to hepatocytes by exploiting different enhancers of transduction, alone or in combination, achieving higher transgene output early after transduction and stably maintained long-term in treated mice. Finally, by coupling the most promising enhancer combination with CD47hi-LV, we further increased transgene output up to 40-fold.

Results

Clonal expansions of LV-transduced hepatocytes progressively increase transgene output without enrichment of LV integrations near cancer genes

To enhance the potency of gene transfer *a posteriori*, we exploited a previously described strategy to endow genetically modified hepatocytes with a selective advantage, as mentioned above[11]. We used vesicular stomatitis virus glycoprotein (VSV.G)-pseudotyped LV expressing codon-optimized human FIX or human FVIII as secreted therapeutic transgenes that could be monitored longitudinally. We used a previously described LV design in which expression of the transgene is tightly hepatocyte-specific[17]. We generated "selectable" LV carrying, next to the transgene, an anti-Cypor shRNA (Supplementary Fig. 1a). We then intravenously (i.v.) administered selectable LV expressing FIX to adult WT mice at two different LV doses. Some of these mice were then intraperitoneally (i.p.) injected with toxic doses of acetaminophen. Liver damage was confirmed by elevation of serum concentrations of alanine aminotransferases (ALT) following acetaminophen injections (Supplementary Fig. 1b). Acetaminophen-treated mice, both in the low LV dose group and in the high LV dose group, showed a positive selection 4–6 weeks after the first acetaminophen doses, as indicated by an increase in FIX amounts over time, compared to non-selected mice, showing stable unchanged FIX amounts (Fig. 1a). The selection was then stopped for 3 months without evidence of a decrease in FIX amounts. Then, to assess if the selection could be resumed on demand, we restarted acetaminophen injections. Mice showed an additional increase in circulating FIX (see Fig. 1a). We achieved a statistically significant 4-fold increase in FIX in selected compared to non-selected mice (Fig. 1b). We then measured LV copies *per* diploid genome (vector copy number, VCN) in the liver after necropsy and in different cell types purified from the liver of treated mice at the end of the experiment: hepatocytes (Hep), liver sinusoidal endothelial cells (LSEC), Kupffer cells (KC, liver resident macrophages), plasmacytoid dendritic cells (pDC) (Supplementary Fig. 1c, d). Consistently with the increased FIX output, we found higher LV VCN in sorted hepatocytes and total liver of selected mice, compared to their counterparts left unselected (Fig. 1c). To confirm the feasibility of the strategy for hemophilia A, we generated selectable LV expressing a non-codon-optimized version of a FVIII transgene to avoid high expression *per* cell. We treated newborn hemophilia A (*F8* knock out, KO) mice with selectable LV-FVIII (see Supplementary Fig. 1a). Some of the mice were then injected with acetaminophen once adults, and liver damage was confirmed by serum ALT elevation (Supplementary Fig. 2a). Selected mice showed progressively increasing circulating FVIII amounts over time, with an ~8-fold increase compared to their un-selected counterparts (Fig. 1d). Importantly, in selected mice, FVIII circulating amounts turned from being sub-therapeutic (3% of normal) to therapeutic (25% of normal). At the end of the experiment, LV VCN was significantly higher in hepatocytes and total liver of selected compared to unselected mice, reflecting the

https://doi.org/10.1038/s41467-025-60073-0

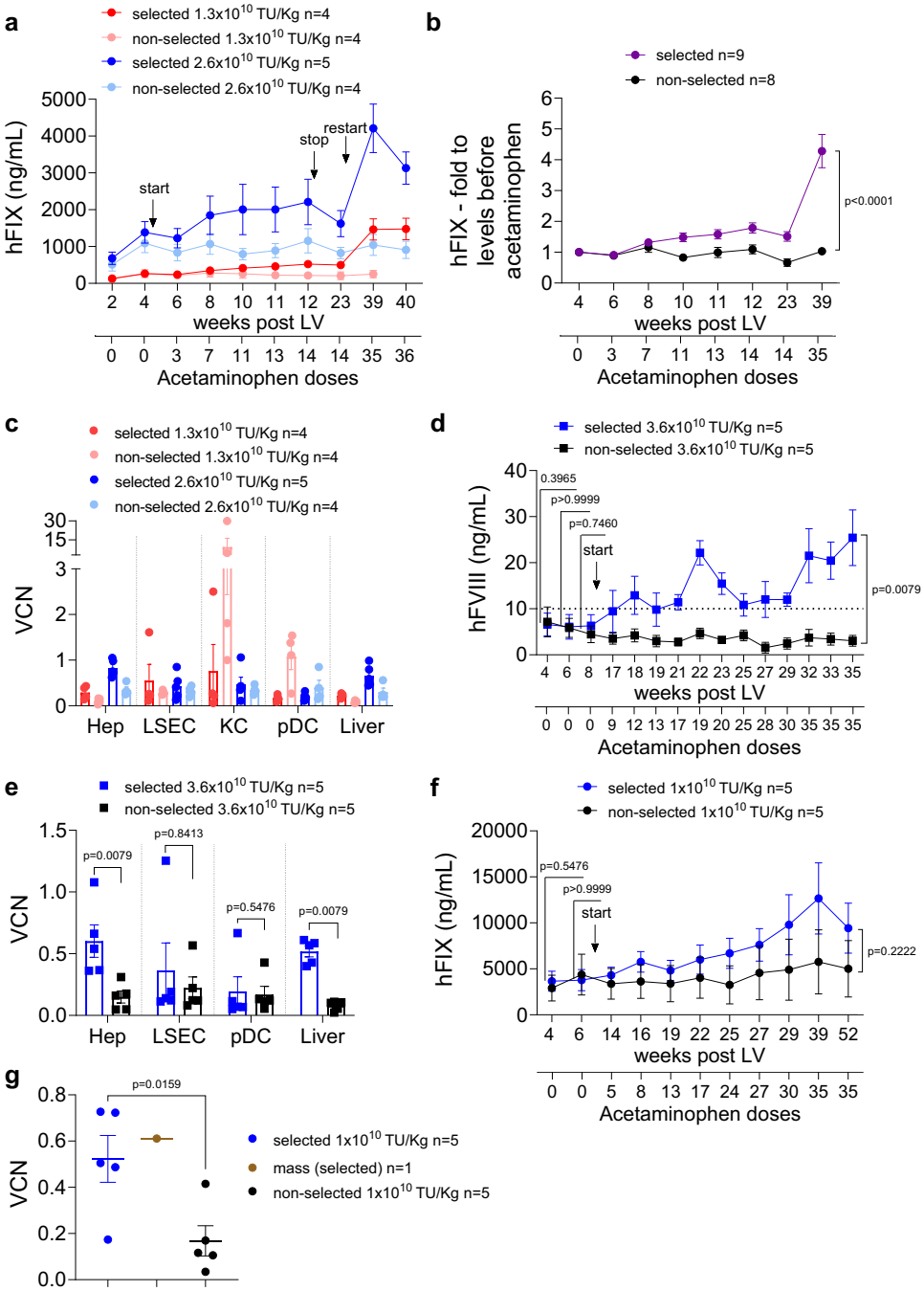

Fig. 1 | Positive selection of transduced hepatocytes allows achieving therapeutically relevant FVIII and FIX amounts. a Mean with standard error of the mean (SEM) of hFIX concentration in the plasma of adult WT mice, treated with LV-shCypor.FIX (1.3×10^{10} or 2.6×10^{10} transducing units, TU/kg) and subjected (blue, red dots), or not (light blue, pink dots) to positive selection of transduced hepatocytes. **b** Mean with SEM of the fold change of hFIX concentration in selected mice (purple dots) and in non-selected controls (black dots), over time, normalized to the hFIX amounts detected on each mouse at the 4 week post-LV time point. Two-tailed Mann-Whitney test (selected vs non-selected at last timepoint) (**c**) Single values and mean with SEM of VCN measured in the fractioned or FACS-sorted liver cell (Hep hepatocytes, LSEC liver sinusoidal endothelial cells, pDC plasmacytoid dendritic cells, KC Kupffer cells) and in the total liver of mice in (**a**), 10 months post-LV. **d** Mean with SEM of hFVIII concentration in the plasma of hemophilia A mice, treated as neonates with LV-shCypor.FVIII (3.6×10^{10} TU/Kg) and subjected (blue dots), or not (black dots) to positive selection of transduced hepatocytes. 10 ng/mL of FVIII (10% of FVIII) is considered the threshold to turn a severe hemophilia phenotype into a mild phenotype[41]. Two-tailed Mann-Whitney test on time points before selection or at the last time point in selected vs non-selected mice. **e** Single values and mean with SEM of VCN measured in the fractioned or FACS-sorted liver cell types and in the total liver of mice in (**d**), 8 months post-LV. Two-tailed Mann-Whitney test. **f** Mean with SEM of hFIX concentration in the plasma of WT mice, treated with LV-shCypor.FIX as 2 week-old (1×10^{10} TU/kg) and subjected (blue dots), or not (black dots), to positive selection of transduced hepatocytes. Two-tailed Mann-Whitney test on time points before selection or at the last time point in selected vs non-selected mice. **g** Single values and mean with SEM of VCN measured in the total liver of LV-treated mice, 1.3 years post-LV. Two-tailed Mann-Whitney test. Source data are provided as a Source Data file.

higher transgene amounts and confirming that expansion was unique to hepatocytes among different liver cell types (Fig. 1e). The same experimental design was applied to 2 week-old mice (Supplementary Fig. 2b), to confirm the feasibility of this strategy at different stages of liver growth. Since the starting FIX circulating amounts were quite high, the selection was more modest (Fig. 1f). Nevertheless, LV VCN in the total liver was significantly higher in selected compared to non-selected mice (Fig. 1g). In one of the selected mice, we found a macroscopic liver mass, diagnosed as hepatocellular adenoma at histopathology analysis, while all other mice in this experiment did not show microscopic liver abnormalities (Supplementary Fig. 2c, d). We measured a VCN of 0.6 in the liver mass, similar to that of the healthy liver counterpart (see Fig. 1g). We mapped genomic LV integration sites (IS). The Shannon Diversity Index was lower in the mass (Supplementary Fig. 2e). Consistently, we found a polyclonal pattern in the healthy tissue and an oligoclonal pattern in the mass, in which an expanded clone represented 35% of the retrieved LV IS (Supplementary Fig. 2f). The dominant LV IS in the mass was located in an intergenic space. Since the integration was not within a gene, and the nearest gene's function is unknown (Supplementary Fig. 2g), it is likely that the transformation of that clone was independent of the LV integration and rather driven by the hepatotoxic regimen the mice were subjected to. Taken together, these data highlight that transduction enhancement can be achieved *a posteriori* by applying a positive selection to transduced hepatocytes. The positive selection was confirmed at the molecular level in two different mouse models treated at different ages.

Since this strategy induces clonal expansions, and we observed a lesion arising in a cohort of selected mice, we set out to compare the distribution of LV genomic IS in selected vs. unselected control mice. To maximize the clonal expansions, we treated adult WT mice with selectable LV-FIX at a very low dose, then selected a fraction of them over time until reaching the circulating FIX amounts obtained in a third group of mice, initially administered with LV-FIX at a 5-fold higher LV dose. Indeed, in this experiment, we achieved up to a remarkable 50-fold increase in FIX output in selected mice compared to non-selected controls, supporting that the lower the starting LV dose, the lower the initial percentage of transduced hepatocytes, the higher the magnitude of the selection that can be achieved (Fig. 2a). The livers of all the mice in this experiment were normal at histopathology analysis (Supplementary Fig. 3a). The VCN in the total liver of the high-dose group was higher than that measured in low-dose non-selected mice. Selected mice showed an intermediate VCN, not reaching values of mice treated at higher starting LV dose, despite showing similar circulating FIX amounts. This is likely due to the contribution of higher VCN in non-parenchymal liver cells in the mice treated with the high LV dose (Fig. 2b). We then performed LV IS analysis in the livers of the above-mentioned groups of mice and retrieved a higher number of unique IS in the high-dose group, as expected (Supplementary Fig. 3b). We found the expected decrease in clonal diversity in mice treated with the low LV dose and then selected, compared to both the other groups, as shown by the percentage of relative abundance of each unique LV genomic IS and the Shannon Diversity Index (Fig. 2c, d and Supplementary Fig. 3c–e). Notwithstanding the clonal expansions, we did not detect any enrichment of LV IS near oncogenes or tumor suppressor genes in the mice that underwent the selection procedure, suggesting that hepatocyte expansions were not driven by LV IS but due to the selective advantage of LV transduced hepatocytes (Fig. 2e). These data suggest that the positive selection procedure did not favor expansions of LV IS near cancer-associated genes. We then specifically assessed the presence of fibrosis and the retention of metabolic zonation in the livers of mice undergoing the selection procedure and unselected controls. We found minimal to mild central fibrosis in mice subjected to selection (Supplementary Fig. 4a–d). We did not observe significant changes in the liver area positive for glutamine synthetase, a marker of peri-central hepatocytes, after the selection procedure (Supplementary Fig. 4e–h). Since the positive selection process required some time to reach therapeutic transgene amounts, which may not be ideal for several genetic conditions, we explored strategies to increase the potency of LV-mediated gene transfer to hepatocytes at the time of LV administration (i.e., a priori).

Transient proteasome or type-I IFN inhibition enhances the potency of in vivo LV gene therapy to hepatocytes

We first determined the effect of transient proteasome inhibition on the efficiency of in vivo hepatocyte transduction by LV in mice. To this end, we used LV expressing codon-optimized human FVIII or codon-optimized human FIX as secreted therapeutic transgenes. Alternatively, we employed LV expressing GFP to visualize transduced hepatocytes at the end of the experiments (Supplementary Fig. 5a). We i.v. administered Bortezomib, a well-known and clinically used proteasome inhibitor, to adult hemophilia B (*F9* KO) mice 1 h before i.v. administration of LV-FIX. The timing of administration was selected based on pharmacokinetic data[18]. We observed ~2-fold higher circulating FIX amounts and activity, stable over time, in mice pre-treated with Bortezomib before LV-FIX compared to control mice (Fig. 3a and Supplementary Fig. 5b). We found similar to slightly lower liver VCN in Bortezomib pre-treated mice (Fig. 3b). We then applied the same protocol for transient proteasome inhibition to adult immune-tolerant hemophilia A mice (*F8* KO, expressing a human mutated non-secreted FVIII, R593C)[19], before administration of LV-FVIII. We confirmed the observation of higher transgene output in Bortezomib pre-treated mice, resulting in stable 10- to 30-fold higher FVIII blood concentration and activity (Fig. 3c and Supplementary Fig. 5c). Note that the different fold changes in FVIII concentration and activity may be due to the lower detection limit of the FVIII activity assay. For this reason, undetectable FVIII amounts may result in detectable FVIII activity, thus likely explaining the observed difference in fold changes. We then measured LV VCN in the different liver cell types. The LV VCN in hepatocytes ranged from 0.1 to 0.4, similar between the two groups (Fig. 3d). Interestingly, LV VCN was almost 5-fold lower in KC and about 2-fold lower in the total liver in mice pre-treated with Bortezomib compared to those treated by LV alone. We repeated the experiment in adult WT mice using LV-GFP and found a statistically significant 2-fold higher GFP-positive liver area in mice administered with Bortezomib before LV (Fig. 3e and Supplementary Fig. 5d, e), without substantial difference in VCN in the total liver (Fig. 3f). These data suggest that the increase in transgene output achieved by transient proteasome inhibition was due to a higher percentage of transduced hepatocytes. We assessed Bortezomib-induced liver toxicity and observed a transient self-limiting increase in serum ALT, no changes in serum aspartate aminotransferases (AST) or alkaline phosphatase (ALP), or increased hepatocyte proliferation (Supplementary Fig. 6), indicating minor self-resolving liver damage, consistent with previous reports[20].

Next, we evaluated the transient inhibition of type-I IFN signaling as a possible transduction enhancer. We administered an anti-IFNAR1 antibody (Ab) or control Ab to adult immune-tolerant hemophilia A mice 3 h before administration of LV-FVIII[21]. We did not detect any difference in FVIII output in mice pre-treated with the control Ab compared to those treated with LV. Conversely, we observed 20-to 40-fold higher FVIII circulating amounts and activity in mice pre-treated with the anti-IFNAR1 Ab (Fig. 4a and Supplementary Fig. 7a). We detected higher, statistically significant LV VCN in hepatocytes and KC (Fig. 4b) in mice receiving anti-IFNAR1 Ab pre-treatment compared to mice receiving LV alone. These data suggest that transient IFNAR1 blockade resulted in higher liver transduction by LV. We then tested if transduction enhancement by Bortezomib was maintained in mice lacking type-I IFN signaling. To this end, we pre-treated *Ifnar*$^{-/-}$ KO mice with Bortezomib before administering LV-FIX. We confirmed a positive effect on FIX transgene output by Bortezomib pre-treatment,

https://doi.org/10.1038/s41467-025-60073-0

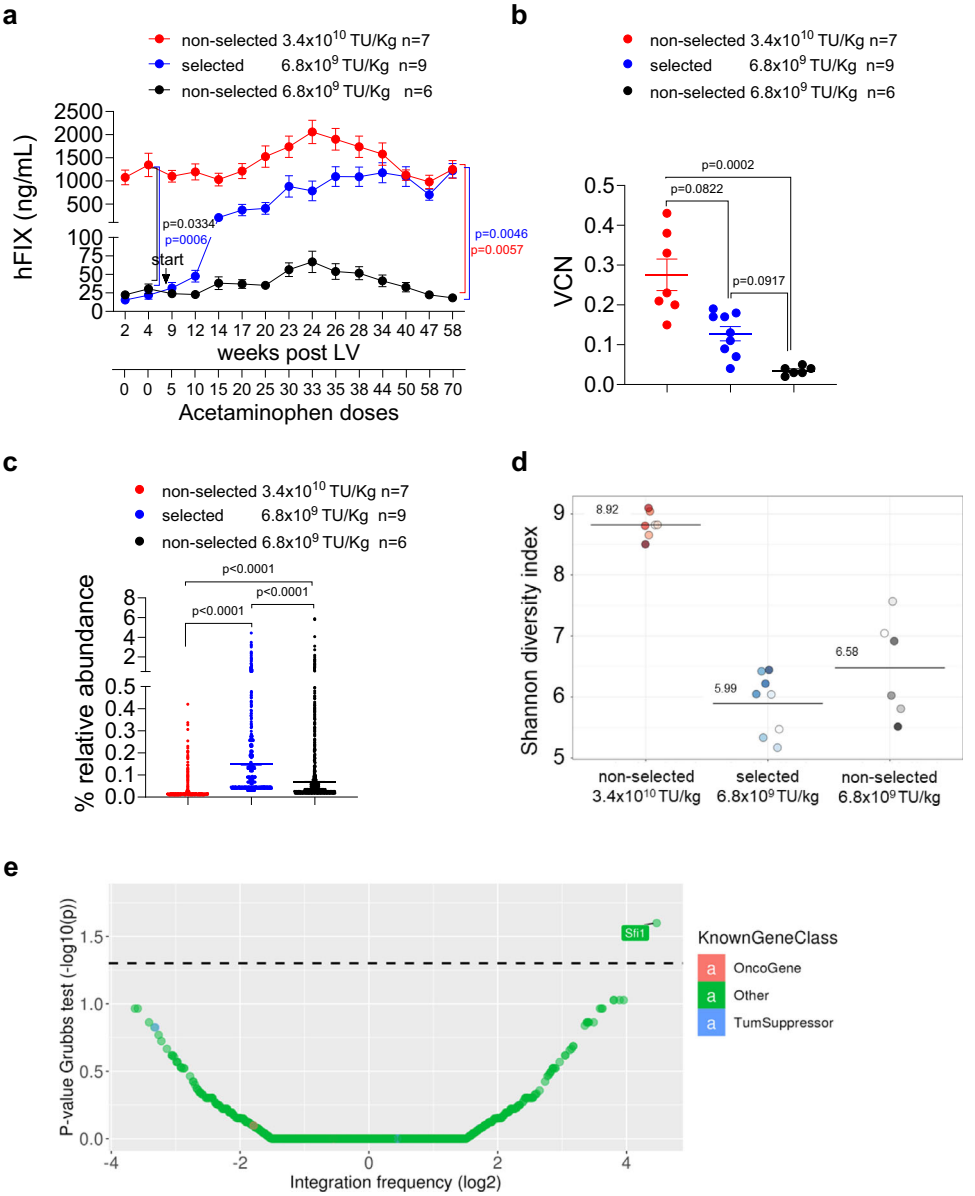

Fig. 2 | Positive selection of LV-transduced hepatocytes is most effective when starting from very low transgene amounts, and does not result in expansion of integrations nearby oncogenes. a Mean with SEM of hFIX concentration in the plasma of adult WT mice, treated with LV-shCypor.FIX (6.8×10^9 or 3.4×10^{10} TU/kg) and subjected (blue dots), or not (black and red dots) to positive selection of transduced hepatocytes. Kruskal-Wallis test with Dunn's multiple comparisons test on time point before selection or at the last time point in selected vs non-selected mice. **b** Single values and mean with SEM of VCN measured in the total liver of LV-treated mice. Kruskal-Wallis test with Dunn's multiple comparisons test. **c** The relative abundance of the integration sites from all mice, split by the specific treatment group, is shown. Bars indicate mean relative abundance values per group. Kruskal–Wallis test with Dunn's multiple comparisons test. **d** The Shannon diversity index of each mouse per specific treatment group is shown as a dot. The average value per group is indicated. **e** Volcano plot of the common IS (CIS), performed on the IS identified in mice treated with 6.8×10^9 TU/kg and subjected to positive selection of transduced hepatocytes. All genes targeted by IS were tested and plotted as dots; gene integration frequency normalized by gene length was placed on the *x*-axis, while the y-axis shows the *p*-value of the CIS Grubbs test for outliers (−log10 of *p*-value). Tumor suppressor genes are annotated in blue, protooncogenes in red, and a generic "other" in green for the remaining genes. Dots with significant *p*-values (α threshold of 0.05) are above the dashed horizontal line. Source data are provided as a Source Data file.

suggesting that the two pathways may be simultaneously targeted to enhance LV transduction further (Supplementary Fig. 7b). We thus pre-treated adult WT mice with Bortezomib and anti-IFNAR1 Ab, alone or in combination, prior to LV-FIX administration. While FIX transgene output was 3-fold higher in Bortezomb pre-treated mice compared to controls, we did not observe any additional benefit by combining Bortezomib and anti-IFNAR1 Ab in this setting (Fig. 4c). These data suggest that doses/timing of the anti-IFNAR1 Ab regimen may be optimized to increase the extent of IFN signaling blockade. We observed a significant reduction of LV VCN in KC and total liver and a tendency of decreased VCN in pDC by Bortezomib pre-treatment, paralleled by an increased VCN in LSEC and a tendency of increased VCN in hepatocytes (Fig. 4d). For this reason, we wondered if the increase in hepatocyte transduction observed following proteasome inhibition was attributable more to an indirect effect, resulting from reduced transduction of liver innate immune cells and more LV available for hepatocytes, or a direct effect on hepatocyte transduction per se. With this purpose, we evaluated whether Bortezomib treatment

https://doi.org/10.1038/s41467-025-60073-0

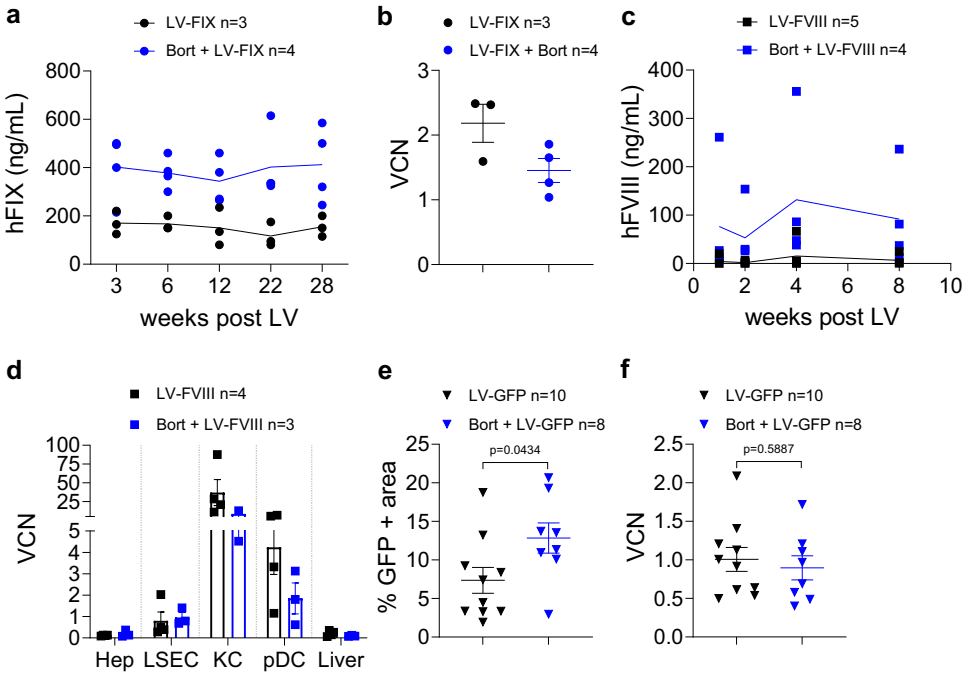

Fig. 3 | Transient proteasome inhibition increases gene transfer to hepatocytes in vivo. a Single values with connecting means of human FIX (hFIX) concentration in the plasma of hemophilia B mice, treated with (blue dots) or without (black dots) Bortezomib (Bort, 1 mg/kg, i.v.) 1 h before LV-FIX (2.5×10^{10} TU/kg). **b** Single values with mean and SEM of VCN measured in the liver of mice in (**a**) 7 months post-LV. **c** Single values with connecting means of human FVIII (hFVIII) concentration in the plasma of immune tolerant hemophilia A mice, treated with (blue squares) or without (black squares) Bortezomib (1 mg/kg, i.v.) 1 h before LV-FVIII (4.5×10^{10} TU/kg). **d** Single values and mean with SEM of VCN measured in fractionated and FACS-sorted liver cell types or in total liver of mice in (**c**) 3 months after LV administration. **e** Single values and mean with SEM of the percentage of GFP-positive liver area in mice treated with (blue triangles) or without (black triangles) Bortezomib (1 mg/Kg, i.v.) 1 h before LV-GFP (2.5×10^{10} TU/kg), analyzed 1 month post-LV. Two-tailed Mann−Whitney test. **f** Single values and mean with SEM of VCN measured in the liver of mice in (**e**) 1 month post-LV. Two-tailed Mann-Whitney test. Source data are provided as a Source Data file.

increases LV transduction in hepatocytes in vitro as well. We transduced human primary hepatocytes with an LV-GFP in the presence or absence of Bortezomib given at the time of transduction. We observed a 2-fold increase in the percentage of GFP-positive hepatocytes and a statistically significant, almost 2-fold increase in VCN when transduction was performed in combination with Bortezomib, as compared to those detected in hepatocytes transduced without Bortezomib (Fig. 4e, f). To exclude the effect of the proteasome inhibitor on the half-life of GFP, Bortezomib was given 2 days after LV transduction (Bort Control), and no increase in the percentage of GFP-positive hepatocytes or VCN was observed in this condition (see Fig. 4e, f). These data indicate that proteasome inhibition also increases LV transduction of hepatocytes by a cell-autonomous mechanism. Overall, these data show that a single administration of a proteasome inhibitor or anti-IFNAR1 Ab enhances the potency of in vivo LV transduction of hepatocytes, with the former being the most efficient, likely through a combined direct and indirect beneficial effect on LV transduction.

Transient fasting improves the potency of in vivo LV gene therapy to hepatocytes

To test if fasting impacted LV transduction, we fasted adult WT mice for 24 h before administration of LV-FIX. We observed ~3-fold higher FIX output, stable over time, in fasted mice compared to non-fasted ones (Supplementary Fig. 8a), while we did not detect any change in LV VCN in the total liver at the end of the follow-up (Supplementary Fig. 8b). The LV dose/kg was defined based on mouse weight before fasting, however, we observed that fasted mice weighed less than their fed counterparts at the time of LV administration (Supplementary Fig. 8c). We thus decided to repeat the experiment including three groups of mice: (i) 8 week-old mice fasted for 24 h, (ii) 8 week-old non-fasted mice, (iii) 6 week-old non-fasted mice (weighting less than the others; Supplementary Fig. 8d). Then, mice were administered with LV-FIX. At the time of LV administration, the weight of fasted 8 week-old mice was overlapping that of 6 week-old mice (Supplementary Fig. 8e). We observed a statistically significant effect of fasting on FIX transgene output (2-fold increase) throughout the follow-up, indicating that higher transduction in the fasted group was not due to higher LV dose/kg at the time of LV administration (Fig. 5a). At the end of the experiment, VCN in sorted hepatocytes was similar in fasted and non-fasted mice (Fig. 5b). However, considering the very high VCN in KC (around 30), even a 1% contamination of KC in hepatocytes may mask changes in the VCN of hepatocytes. Thus, we set out to assess whether fasting increased the LV-transduced liver area. To this end, we exploited an LV construct co-expressing FIX and GFP (LV-FIX IRES GFP; Supplementary Fig. 8f). We confirmed the higher transgene output in fasted mice with this LV (Fig. 5c) and observed a higher percentage of GFP-positive tissue area (Fig. 5d and Supplementary Fig. 8g, h) and RNA derived from LV (Fig. 5e) in fasted mice, compared to non-fasted counterparts, reflecting higher hepatocyte transduction in the former, despite comparable VCN in the total liver (Fig. 5f). We performed an additional experiment using LV expressing GFP exclusively and found a statistically significant 1.5-fold higher GFP-positive liver tissue area in fasted compared to non-fasted mice (Fig. 5g), with similar VCN in the total liver (Fig. 5h). Altogether, these data indicate that 1 day of fasting enhanced the potency of in vivo hepatocyte transduction and transgene output by LV in mice.

In an effort to understand the reasons behind higher gene transfer in fasted mice, we determined the effect of fasting on the low-density

https://doi.org/10.1038/s41467-025-60073-0

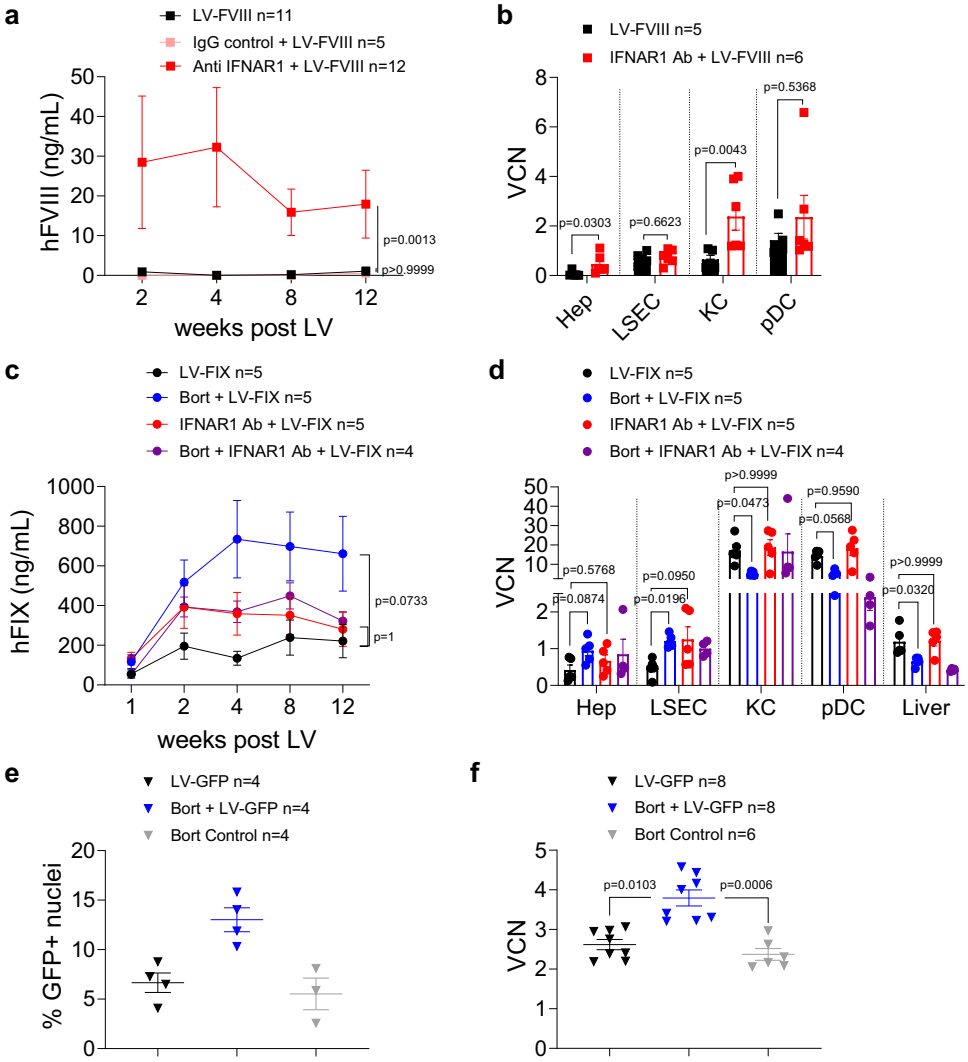

Fig. 4 | Transient IFN signaling inhibition increases gene transfer to hepatocytes in vivo without additional advantage if combined with Bortezomib. **a** Mean with SEM of hFVIII concentration in the plasma of immune tolerant hemophilia A mice, treated with (red squares) or without (black squares) anti-IFNAR1 Ab (50 mg/kg, i.v.) or with a control Ab (immunoglobulin G control, IgG control, pink squares) 3 h before LV-FVIII ($4–7 \times 10^{10}$ TU/kg). Pool of two independent experiments. Kruskal-Wallis test with Dunn's multiple comparisons test over LV-FVIII control group, performed at the last time-point. **b** Single values and mean with SEM of VCN measured in the indicated fractionated or FACS-sorted liver cell types of mice in (**a**) 5 months post-LV. Two-tailed Mann-Whitney test. **c** Mean with SEM of hFIX concentration in the plasma of WT mice, treated with Bortezomib (1 mg/kg, blue dots) and/or Anti-IFNAR1 Ab (50 mg/kg, purple or red dots, as indicated) or saline (black dots), 1 h or 3 h before LV-FIX (2.75×10^{10} TU/kg). Two-tailed linear-mixed effects (LME) model (for complete analyses see Supplementary Table 1) over LV-FIX group. **d** Single values and mean with SEM of VCN measured in fractionated and FACS-sorted liver cell types of mice in (**c**) 3 months post-LV. Kruskal-Wallis test with Dunn's multiple comparisons test over LV-FIX control group. **e** Single values and mean with SEM of the percentage of GFP-positive hepatocytes (7 fields/sample) transduced with PGK.GFP LV (multiplicity of infection (MOI): 2), in the presence (blue triangles) or absence (black triangles) of Bortezomib (100 nM) at the time of transduction, and analyzed 7 days after transduction. As a control for inhibition of GFP degradation, Bortezomib (100 nM) was added 2 days after LV administration (condition Bort control, gray triangles). **f** Single values and mean with SEM of VCN measured in the above-described experiment. Kruskal-Wallis test with Dunn's multiple comparisons test. Source data are provided as a Source Data file.

lipoprotein receptor (LDLR) pathway since LDLR and its family members are known to be bound by VSV.G to mediate LV entry[22,23]. Groups in the experiment were the following: (i) control adult mice fed *ad libitum*, (ii) adult mice fasted for 12 h, (iii) adult mice fasted for 24 h, (iv) adult mice fasted for 24 h, then re-fed for 24 h (Supplementary Fig. 9a). Circulating amounts of Proprotein convertase subtilisin/kexin type 9 (PCSK9), a negative modulator of LDLR were reduced over time during fasting (Supplementary Fig. 9b). *Ldlr* expression was reduced in the liver of fasted mice, following the same trend as PCSK9 (Supplementary Fig. 9c), while the expression of most *Ldlr* family members did not change (Supplementary Fig. 9d–i). Interestingly, the reduction of *Ldlr* RNA over fasting suggests that lower LDLR amounts improve rather than impair LV transduction in vivo in the liver. Thus, we evaluated the liver gene transfer efficiency by LV-FIX in adult *Ldlr* KO mice, completely lacking LDLR. Remarkably, *Ldlr* KO mice showed 2-3.5-fold higher circulating FIX amounts than WT mice, bearing a functional LDLR, at both LV doses tested (Fig. 6a). The LV VCN in KC, pDC, and total liver were comparable between the two strains, while VCN in LSEC was higher in *Ldlr* KO mice (Fig. 6b). We observed a tendency towards an increase of VCN in sorted hepatocytes in *Ldlr* KO mice (see Fig. 6b) and did not detect any LV RNA in LSEC, as expected (Fig. 6c). We tested if the LDLR family members were upregulated in a compensatory fashion, in response to the lack of LDLR. However, we did not observe any difference in the hepatic expression of *Ldlr* family members in *Ldlr*

https://doi.org/10.1038/s41467-025-60073-0

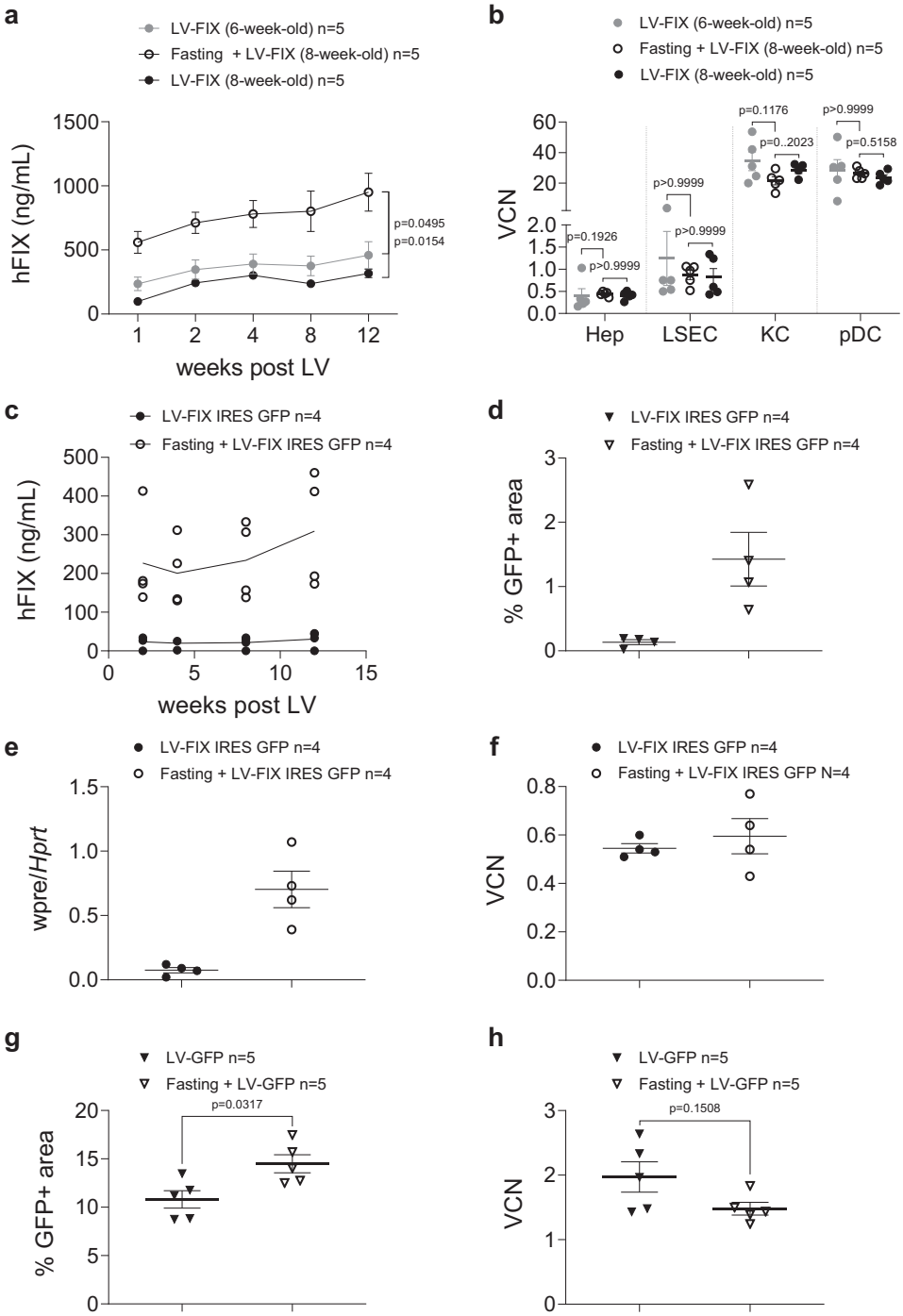

Fig. 5 | One day of fasting increases gene transfer to hepatocytes in vivo. a Mean with SEM of hFIX concentration in the plasma of adult WT mice, fasted 24 h (empty black dots) or fed *ad libitum* (6 week-old, gray dots, 8 week-old, black dots) before LV-FIX (4×10^{10} TU/kg). Two-tailed linear-mixed effects (LME) model (for complete analyses see Supplementary Table 3) over Fasting + LV-FIX 8 week-old group. **b** Single values and mean with SEM of VCN measured in fractionated and FACS-sorted liver cell types of mice in (**a**) 3 months after LV administration. Kruskal-Wallis test with Dunn's multiple comparisons test over fasted mice. **c** Mean with SEM of hFIX concentration in the plasma of adult WT mice, fasted 24 h (empty black dots) or fed *ad libitum* (black dots) before LV-FIX IRES GFP (2×10^{10} TU/kg). **d** Single values and mean with SEM of the percentage of GFP-positive liver area of mice in (**c**), 3 months post-LV. **e** Single values and mean with SEM of wpre expression (proxy of LV transgene), normalized on the endogenous *Hprt* gene, in the livers of mice in (**c**). **f** Single values and mean with SEM of VCN measured in the total liver of mice in (**c**). **g** Single values and mean with SEM of the percentage of GFP-positive liver area of mice adult WT mice, fasted 24 h (empty triangles) or fed *ad libitum* (black triangles) before LV-GFP (2.5×10^{10} TU/kg), 1 week post-LV. Two-tailed Mann-Whitney test. **h** Single values and mean with SEM of VCN measured in the total liver of mice in (**g**). Two-tailed Mann–Whitney test. Source data are provided as a Source Data file.

KO mice (Fig. 6d). To confirm the result observed with the FIX transgene and to visualize LV-transduced cells, we moved to LV-GFP. We observed 5.6% of GFP-positive liver area in *Ldlr* KO compared to 3.5% in WT mice, supporting that the higher transgene output observed before was likely due to an increased transduced liver area (Supplementary Fig. 9j–l). These data show that fasting improves the efficiency of LV gene transfer into hepatocytes, possibly by reducing hepatic LDLR expression.

https://doi.org/10.1038/s41467-025-60073-0

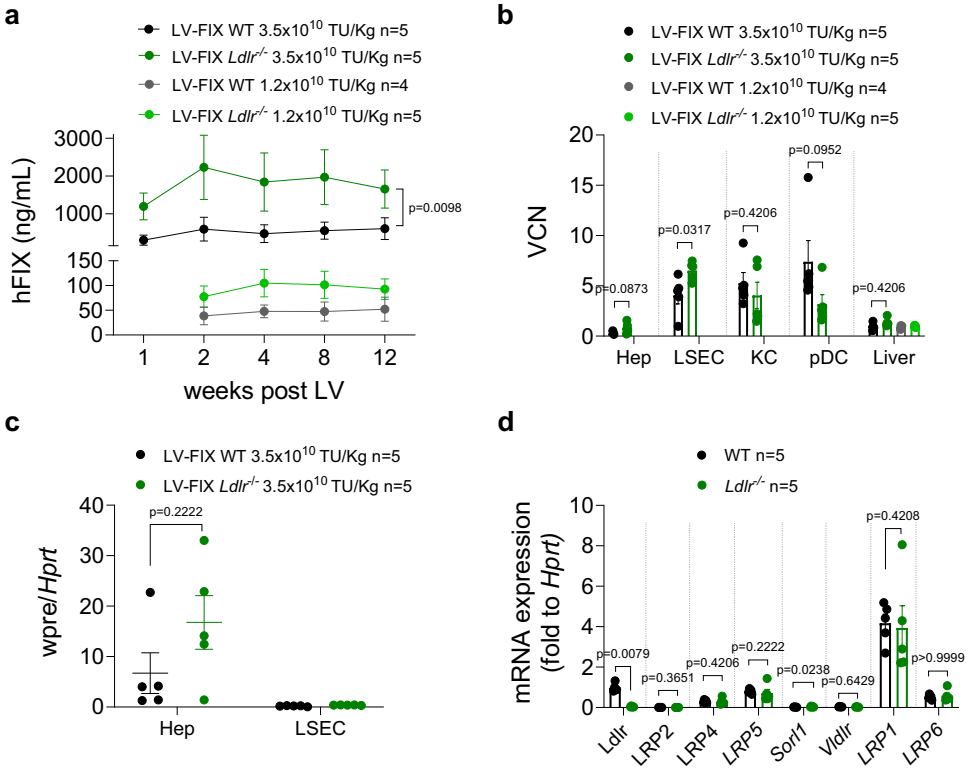

Fig. 6 | *Ldlr*$^{-/-}$ hepatocytes are transduced by LV at higher efficiency compared to WT mice in vivo. a Mean with SEM of hFIX concentration in the plasma of adult WT (black and gray dots) or *Ldlr*$^{-/-}$ mice (dark and light green dots) treated with LV-FIX (3.5×10^{10} TU/kg or 1.2×10^{10} TU/kg). Two-tailed linear-mixed effects (LME) model (for complete analyses see Supplementary Table 4). **b** Single values and mean with SEM of VCN measured in fractioned or FACS-sorted liver cell types or in the total liver of mice in (**a**), 3 months post-LV. Two-tailed Mann–Whitney test. **c** Single values and mean with SEM of WPRE expression (proxy of LV transgene), normalized on the endogenous *Hprt* gene, in sorted hepatocytes or sorted LSEC of mice in (**a**). Two-tailed Mann-Whitney test. **d** Single values and mean with SEM of expression of *Ldlr* and *Ldlr* family members genes, normalized on the endogenous *Hprt* gene, in the livers of adult WT or *Ldlr*$^{-/-}$ mice. Two-tailed Mann-Whitney test. Source data are provided as a Source Data file.

Combining transduction enhancers and engineered phagocytosis-shielded LV maximizes in vivo gene transfer efficiency to hepatocytes

Once we identified three different enhancers of transduction (Bortezomib, anti-IFNAR1 Ab, and fasting), we assessed whether we could achieve an additive or even synergistic effect by combining them in WT or *Ldlr* KO adult mice. Fasting as a single treatment provided the most prominent advantage in WT mice, where transgene amounts were ~7-fold higher than in control mice treated with LV-FIX alone (Fig. 7a). Moreover, the combination of fasting and anti-IFNAR1 Ab or fasting and Bortezomib further improved the outcome, reaching up to ~13-fold higher circulating FIX amounts than in LV-only control mice (see Fig. 7a). In line with the previous observation about the lack of additive effect of Bortezomib and anti-IFNAR1 Ab (see Fig. 4c), even when the two drugs were combined with fasting, we did not observe any further increase in FIX output compared to the combination of fasting and each single agent. Interestingly, we observed a milder effect of the fasting procedure on transgene output in *Ldlr* KO compared to WT mice, suggesting that the enhancement of LV transduction obtained by the fasting protocol is due, at least in part, to the downregulation of the LDLR in the liver (see Fig. 7a). Even in *Ldlr* KO mice, the greatest advantage was achieved by combining fasting with Bortezomib. There was no detectable difference in VCN in the total liver among experimental groups (Fig. 7b). We repeated the most promising enhancer combination (fasting and Bortezomib) in WT mice before the administration of LV-FIX. We confirmed a statistically significant increase in FIX output, stably maintained throughout the follow-up, by each single treatment and achieved an overall 11-fold increase (Fig. 7c), similar to what was previously observed (see Fig. 7a). At the end of the follow up we measured the VCN in sorted hepatocytes from the livers of experimental mice and observed values on average 1.5-fold, 2-fold or 3.5-fold higher in mice pre-treated with fasting, bortezomib or both, respectively, compared to mice treated with LV only (Fig. 7d). Importantly VCN in sorted hepatocytes positively correlated with FIX transgene output, confirming transduction enhancement (Supplementary Fig. 10a). Additionally, we confirmed a higher VCN in sorted LSEC of mice pre-treated with Bortezomib (Fig. 7e), as seen before (see Fig. 4d). We also confirmed a positive effect on FVIII transgene output by fasting and anti-IFNAR1 blockade in adult immune-tolerant hemophilia A mice (Supplementary Fig. 10b). Finally, we assessed a possible additive or synergistic effect of transduction enhancers when combined with CD47hi-LV-FIX in NOD mice, in which the CD47 receptor cross-reacts with the human ligand present on the LV surface[7,24]. We observed a statistically significant increase in FIX transgene output in mice receiving fasting and anti-IFNAR1 Ab or with fasting and Bortezomib before vector administration (Fig. 7f). Notably, by employing fasting and Bortezomib, we observed >40-fold higher FIX transgene output than in control mice treated with CD47hi-LV-FIX alone. When the same combination was tested with LV-FIX, WT mice showed up to 13-fold higher transgene output. Altogether, these data show that several minimally invasive procedures, alone or in combination, before LV administration can be employed to maximize in vivo hepatocytes' transduction a priori and highlight a possible synergistic effect of the identified transduction enhancers when combined with phagocytosis-shielded LV.

Discussion

We report here that several different interventions could be employed in the setting of in vivo gene therapy to enhance the potency of LV

https://doi.org/10.1038/s41467-025-60073-0

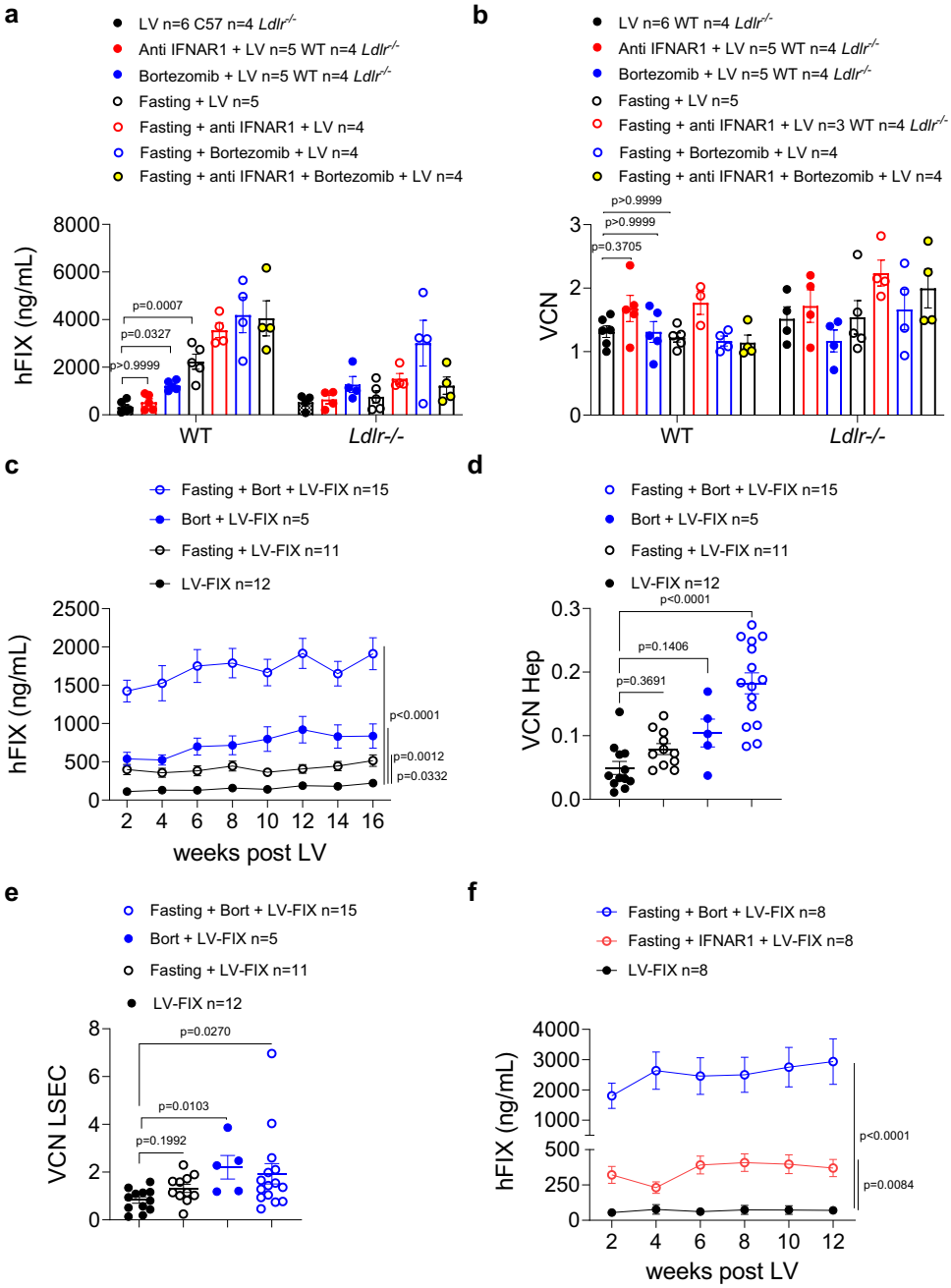

Fig. 7 | Combinations of the previously identified transduction enhancers further improve gene transfer efficiency to hepatocytes in vivo. a Single values and mean with SEM of hFIX concentration in the plasma of LV-FIX treated mice (average of 4 time points: 15, 20, 26, 46 weeks post-LV). WT and *Ldlr*$^{-/-}$ mice were either administered with LV-FIX (black dots, 2.75×10^{10} TU/kg) or pre-treated with Anti-IFNAR1 Ab (50 mg/kg, i.v., red dots) or with Bortezomib (1 mg/kg, blue dots) or fasted for 24 h (empty black dots), or fasted and pre-treated with Anti-IFNAR1 Ab (empty red dots), or fasted and pre-treated with Bortezomib (empty blue dots), or fasted and pre-treated with Anti-IFNAR1 and Bortezomib, before LV-FIX (2.75×10^{10} TU/kg). Kruskal-Wallis test with Dunn's multiple comparisons test over LV-FIX control group. **b** Single values and mean with SEM of VCN measured in the total liver of mice in (**a**). Kruskall-Wallis test with Dunn's multiple comparisons test over LV-only group. **c** Mean with SEM of hFIX concentration in the plasma of LV-FIX treated mice. WT mice were either administered with LV-FIX (black dots) or pre-treated with Bortezomib (blue dots) or fasted for 24 h (empty black dots), or fasted and pre-treated with Bortezomib (empty blue dots), before LV-FIX (1.8×10^{10} TU/kg). Two-tailed linear-mixed effects (LME) model (for complete analyses see Supplementary Table 5), over LV-FIX group. **d** Single values and mean with SEM of VCN measured in the sorted hepatocytes of mice in (**c**). Kruskal–Wallis test with Dunn's multiple comparisons test over LV-only group. **e** Single values and mean with SEM of VCN measured in the sorted LSEC of mice in (**c**). Kruskal–Wallis test with Dunn's multiple comparisons test over LV-only group. **f** Mean with SEM of hFIX concentration in the plasma of CD47hi-LV-FIX treated mice. NOD mice were either administered with CD47hi-LV-FIX (black dots), fasted and pre-treated with anti-IFNAR1 Ab (empty red dots) or fasted and pre-treated with Bortezomib (empty blue dots), before CD47hi-LV-FIX (1.4×10^{10} TU/kg). Two-tailed linear-mixed effects (LME) model (for complete analyses see Supplementary Table 6), over LV-FIX group. Source data are provided as a Source Data file.

transduction of hepatocytes in several mouse models and using different transgenes. We augmented the efficiency of LV-mediated gene transfer into hepatocytes by targeting known anti-viral pathways, thus overcoming some of the restrictions limiting the potential of in vivo viral vector transduction. We achieved this transduction enhancement by inhibition of proteasome activity, type-I IFN signaling, or through a fasting regimen. Although transient, all these procedures allowed obtaining a higher gene transfer, resulting in a stable, long-term

increase in transgene output and therapeutic efficacy in two disease models. We observed a stronger fold increase in FIX than GFP, in the presence of transduction enhancers, likely due to codon optimization of the former, resulting in high expression and secretion by each transduced hepatocyte, thus amplifying the increase in the transduced liver area observed with the GFP transgene. The difference in fold increase was even more evident with FVIII as a transgene, which was codon-optimized to maximize production *per* cell[8]. The effect of the anti-IFNAR1 Ab was less pronounced with the FIX transgene than with the FVIII transgene. This outcome may be due to the higher LV doses administered and the longer genome in FVIII-carrying LV than in FIX-carrying LV, thus potentially explaining a stronger effect of blocking IFN signaling with the former LV.

When LV-transduced hepatocytes were positively expanded *a posteriori*, the increase in transgene output was reflected by an increase in VCN in purified hepatocytes and total liver, while no major differences were observed in the VCN of other liver cell types, indicating that, despite initial transduction of multiple cell types in the liver, the expansion was selective for hepatocytes. Conversely, transduction enhancement a priori was not always accompanied by a detectable increase in VCN of hepatocytes or total liver because the VCN in total liver results from the weighted average of the VCN in different liver cell types, as previously described[7]. In Bortezomib-treated mice, the increase of LV gene transfer into hepatocytes may be due to a skewed distribution of LV among liver cell types, as noted by the generally lower VCN in KC and pDC. Improvement of LV transduction of hepatocytes by Bortezomib may indeed be due to both a cell-intrinsic and non-cell-intrinsic mechanism, as shown by increased transduction of primary hepatocytes. IFNAR1 inhibition likely exerted a more direct effect on hepatocytes, as shown by the increase in LV VCN in these cells. In the case of fasting, the very high VCN in KC in adult WT mice may be masking an increase in VCN of sorted hepatocytes, in which 1% contaminating KC is present. Indeed, this procedure resulted in a higher transgene-positive liver area, thus supporting gene transfer in a larger proportion of hepatocytes. Nevertheless, when transduction enhancement was more pronounced, such as in the presence of multiple enhancers, we observed a significant increase in VCN of sorted hepatocytes, directly correlating with transgene output. Interestingly, Bortezomib pretreatment also increased LV transduction of LSEC, the natural site of FVIII production, which may also be exploited for other gene therapy applications[25].

The lack of synergy of proteasome and IFN signaling inhibition, together with the better outcome obtained with the former compared to the latter, suggest that Bortezomib increases gene transfer impacting the IFN pathway as well. Indeed, it has been shown that Bortezomib reduces both the function and survival of pDC, the major producers of type-I IFN[26]. Thus, while IFNAR1 inhibition may render hepatocytes insensitive to IFN signaling, Bortezomib may indirectly diminish IFN signaling by transiently reducing the functionality of their cellular source, consequently improving hepatocyte transduction. However, the positive effect of Bortezomib on LV gene transfer was maintained in *Ifnar* KO mice, further supporting a dual mechanism of hepatocyte transduction enhancement. Surprisingly, decreased liver expression or even the absence of LDLR increased rather than decreased LV transduction of hepatocytes. The LDLR family members, highly expressed by hepatocytes, may allow for more efficient LV transduction than the LDLR itself. Indeed, transduction enhancement by fasting may be due, at least in part, to LDLR reduction. This is supported by the observation that the effect of fasting on LV transduction was less pronounced in *Ldlr* KO mice. Endocytosis and vesicular transport inside hepatocytes with lower or absent LDLR may be altered in such a way as to favor the entry and trafficking of LV particles, ultimately improving LV transduction efficiency. However, since fasting has pleiotropic effects on hepatocyte metabolism, we cannot exclude that other pathways, such as autophagy, have a role in this positive outcome.

All the proposed strategies to enhance LV transduction a priori are transient (fasting) or single-dose and potentially clinically applicable: (i) Bortezomib (Velcade) is a clinically approved proteasome inhibitor used as a chronic therapy in patients affected by multiple myeloma[27]; (ii) Anifrolumab (Saphnelo) is an anti-IFNAR1 monoclonal Ab, used in cases of moderate-to-severe systemic lupus erythematosus[28]; (iii) a 1-day fasting procedure is feasible in humans and with kinetics of PCSK9 reduction similar to that shown in mice[29], supporting that the same fasting time may be applied to obtain similar effect on LDLR pathway. We observed a Bortezomib-induced transient minor liver damage, in line with previous reports[20]. Concerning type-I IFN blockade, it would be important to avoid vaccines made of attenuated pathogens in the month following Saphnelo administration. The reported Saphnelo-related side effects, such as a higher frequency of infections, are likely due to repeated exposures to the drug[30]. In any case, further pre-clinical investigations on the use of transduction enhancers together with in vivo LV gene therapy will be necessary before clinical evaluation.

We validated the strategy of positive selection of genetically corrected hepatocytes, previously shown to be effective in neonatal mice[11], at different ages of treatment and using different transgenes. In addition, we show that selection can be halted and resumed on demand. We highlight the translational potential as well as the challenges of expanding LV-transduced hepatocytes *a posteriori*, exposing untransduced cells to toxicity, thus increasing the risk of tumoral development. Whereas therapeutic efficacy can be achieved by low starting LV doses, potentially reaching a predefined transgene amount, a prolonged time may be necessary to reach the desired outcome, which is not always compatible with the medical condition. In addition, resistance to acetaminophen toxicity may occur following repeated exposure to the drug, thus requiring continuously increasing acetaminophen dosage to induce liver damage[31,32]. Therefore, it may be challenging to apply this strategy to specific metabolic diseases at risk of fatal metabolic decompensations. Notwithstanding that this strategy implies clonal expansions of LV-transduced hepatocytes, we did not detect preferential expansions of clones harboring LV integrations near oncogenes. However, a hepatocellular adenoma arose in a cohort of mice that underwent the selection procedure with an initially high liver transduction efficiency, possibly due to exposure to chronically high acetaminophen doses. Furthermore, restoring CYPOR activity, once the selection is completed, would be preferable for potential clinical application. Enhancing the potency of liver gene transfer a priori by exploiting transduction enhancers may allow an improved therapeutic outcome soon after gene therapy, still saving on the LV doses required for efficacy. Moreover, a higher percentage of transduced hepatocytes upon gene therapy may be beneficial for establishing immune tolerance to the transgene product, favored by the pro-tolerogenic liver environment[33]. This aspect may be particularly relevant in the case of highly immunogenic transgenes such as FVIII.

When we tested the three transduction enhancers in combination, we identified 24 h of fasting and Bortezomib administration before LV as the combination achieving the highest gene transfer, suggesting an additive effect of the two pathways. Furthermore, when we coupled this combination to phagocytosis-shielded LV, we attained a remarkable 40-fold increase in FIX transgene output. This outcome indicates a successful synergy between the phagocytosis protection mediated by high CD47 amounts in LV particles, resulting in higher LV bioavailability for hepatocytes and the concomitant release of restrictions to their efficient transduction. Transduction enhancement a priori and *a posteriori* may be exploited together to minimize LV doses and the acetaminophen administrations required to reach therapeutic efficacy.

Overall, our work highlights the translational potential of a minimally invasive, cost-effective combination of treatments, which could be employed together with LV to enhance the potency of in vivo gene therapy to hepatocytes, enabling to tackle new and more challenging diseases requiring a high percentage of hepatocyte transduction. Increasing the potency of gene transfer remains a crucial goal in gene therapy since lowering the dose required to achieve therapeutic efficacy would decrease dose-dependent toxicities and immunogenicity, besides reducing the costs associated with manufacturing. We successfully enhanced the potency of in vivo LV-mediated hepatocyte gene transfer, thus paving the way to expanding its in vivo applicability and easing its clinical translation.

Methods

Mice experiments

All animal experiments were carried out under good animal practices following Italian and European legislation on animal care and experimentation (2010/63/EU). All animal procedures were performed according to protocols approved by the Institutional Animal Care and Use Committee and the Italian Ministry of Health. B6;129S-*F8*tm1Kaz/J mice (referred to as HemoA or *F8* KO) were obtained from Jackson Laboratories (stock #004424). *F8*tm1Kaz Tg(Alb-F8*R593C)T4Mcal/J mice (referred to as HemoA-R593C) were obtained from The Jackson Laboratories (stock #017706). B6;129P2-F9tm1Dws/J mice (referred to as HemoB or *F9* KO) were obtained from Jackson Laboratories. C57BL/6NCrl mice were purchased from the Charles River Laboratories. B6;129S-LdlrTm1Her/J (referred to as $Ldlr^{-/-}$ or LDLR KO) were obtained from Jackson Laboratories (stock #002207). Mice defective for type-I IFN receptor 129/SVEV ($Ifnar^{-/-}$) were obtained from B&K Universal Limited. NOD mice were purchased from the Charles River Laboratories. All mice were kept in specific pathogen-free conditions and fed *ad libitum*, with the exception of in case of fasting, with VRF1 (P) by Special Diet Services. LV was administered to adult mice, males and females (6–10 weeks of age), through either tail vein or retro-orbital plexus (250–500 µL/mouse). LV was administered in newborn mice, males or females, through the temporal vein (25–30 µL/mouse). LV was administered in juvenile mice (2 weeks of age), males or females, through retro-orbital plexus (100–200 µL/mouse). Mice were bled from the retro-orbital plexus through capillary tubes. Blood was collected in 0.38% sodium citrate buffer, pH 7.4. Mice were euthanized by cervical dislocation at the scheduled time. For fasting experiments, the weight used to calculate LV dose/kg was measured before starting the fasting procedure. Males or female mice were starved for the number of hours indicated and then treated or not with LV. Over fasting time, the mice were injected twice, i.p., with saline. For experiments with Bortezomib (Velcade), the drug (1 mg/kg) was administered, once diluted in saline, i.v. 1 h before LV administration. For experiments with MarI (anti-IFNAR1 Ab, clone MARI-5A3, Merk), the drug (50 mg/kg) was administered, once diluted in saline, i.v. 3 h before LV administration. For experiments with mouse IgG1 isotype control, the antibody (MOPC-21, Bioxell), was administered, once diluted in saline, i.v. 3 h before LV administration. The experiments were not blinded to the sample code. We processed samples blind to the sample code only for histopathological analysis up to the stage of data analysis. We reported the experiments involving animals following the ARRIVE guidelines.

Plasmid construction

Plasmids used for this work were either already available in the lab, or they were generated through standard cloning techniques, inserting into backbones, already available, inserts derived from other pre-existing plasmids or derived from gene synthesis required ad hoc. LV *U6-Cypor-shRNA-ET-hFVIII-wpre** was generated starting from LV *U6-Cypor shRNA-co.FIX* sequence[11], used as backbone. The co.*FIX* transgene was replaced with *FVIII* deriving from LV-*FVIII*[6].

Plasmid DNA purification

Large-scale amounts of plasmids DNA, required during vector generation, were obtained using Machaery-Nagel-endotoxin-free high-purity plasmid maxi preparation system. Purification was performed following the manufacture's instructions. Plasmids were subsequently resuspended in TE (10 mM TrisHCl, pH8, 1 mM EDTA). Packaging and envelope plasmids were generated by Nature Technology Corporation. Small-scale amounts of plasmids DNA, required during the screening of colonies following cloning, were obtained using Wizard® Plus SV Minipreps DNA Purification System (Promega).

Vector production

Third-generation self-inactivating (SIN) LV were produced by calcium phosphate transient transfection into 293 T cells. 293 T cells were transfected with a solution containing a mix of the selected LV genome transfer plasmid, the packaging plasmids pMDLg/pRRE and pCMV.REV, pMD2.G and pAdVantage (Promega), as previously described[7]. Briefly, the medium was changed 14–16 h after transfection, and the supernatant was collected 30 h after the medium change. LV-containing supernatants were sterilized through a 0.22 µm filter (Millipore), transferred into sterile poliallomer tubes (Beckman) and centrifuged at 20,000 g for 120 min at 20 °C (Beckman Optima XL-100K Ultracentrifuge). For FVIII transgene encoding LV, before centrifugation, LV-containing 0.22 µm-filtered supernatants were pre-concentrated 4 times with Vivaflow 200 Tangential Flow Filtration Cassette 100 kDa (Sartorius), according to manufacturing instructions. LV pellet was dissolved in the appropriate volume of PBS to allow 500–1000X concentration.

LV titration

For LV titration, 1×10^5 293 T cells were transduced with serial LV dilutions in the presence of polybrene (8 µg/ml). Genomic DNA (gDNA) was extracted 14 days after transduction, using Maxwell 16 Cell DNA Purification Kit (Promega), following the manufacturer's instructions. VCN was determined by droplet digital PCR (ddPCR), starting from 5–20 ng of template gDNA using primers (HIV fw: 5′-TACTGACGCTCTCGCACC-3′; HIV rv: 5′-TCTCGACGCAGGACTCG-3′) and a probe (FAM 5′-ATCTCTCTCCTTCTAGCCTC-3′) designed on the primer binding site region of LV. The amount of endogenous DNA was quantified by a primers/probe set designed on the human telomerase gene (Telo fw: 5′-GGCACACGTGGCTTTTCG-3′; Telo rv: 5′-GGTGAACCTCGTAAGTTTATGCAA-3′; Telo probe: VIC 5′-TCAGGACGTCGAGTGGACACGGTG-3′ TAMRA) or the human GAPDH gene (Applied Biosystems HS00483111_cm). The PCR reaction was performed with each primer (900 nM) and the probe (250 nM, 500 nM for Telo) following the manufacturer's instructions (Biorad), read with QX200 reader, and analyzed with QuantaSoft software (Biorad). Infectious titer, expressed as TU/mL, was calculated using the formula TU/mL = (VCN x 100,000 x (1/dilution factor).

VCN determination

For the experiment with primary hepatocytes, DNA was extracted using DNeasy Blood & Tissue Kit (Qiagen), following the manufacturer's instructions. For mice experiments, DNA was extracted from whole liver samples using Maxwell 16 Tissue DNA Purification Kit (Promega), DNA was extracted from fractionated/sorted liver cells using DNeasy Blood & Tissue Kit (Qiagen) or QIAamp DNA Micro Kit (Qiagen), according to cell number. VCN in murine DNA line was determined by ddPCR, starting from 5–20 ng of template gDNA using a primers/probe set designed on the primer binding site region of LV (see "LV titration" above). For primary hepatocytes, VCN was determined using an ad hoc qPCR, which selectively amplifies the reverse transcribed vector genome (both integrated and non-integrated) discriminating it from plasmid carried over from the transient transfection (RT-LV; ΔU3 fw: 5′-TCACTCCCAACGAAGACAAGATC-3′, gag rv: 5′-

GAGTCCTGCGTCGAGAGAG-3′)[34]. The amount of endogenous DNA was quantified by primers set designed on the human telomerase gene, as above, or the murine Sema3A gene, as described below. The amount of endogenous murine DNA was quantified by a primers/probe set designed on the murine sema3a gene (Sema3A fw: 5′-ACCGATTCCAGATGATTGGC-3′; Sema3A rv: 5′-TCCATATTAATGCAGTGCTTGC-3′; Sema3A probe: HEX 5′-AGAGGCCTGTCCTGCAGCTCATGG-3′ BHQ1). The PCR reaction was performed with each primer (900 nM, 150 nM for RT-LV primers) and the probe (250 nM) following manufacturer's instructions (Biorad), read with QX200 reader and analyzed with QuantaSoft software (Biorad).

Cell cultures and in vitro experiments

293 T cells were maintained in Iscove's modified Dulbecco's medium (IMDM, Gibco 21980-032) with additive L-Glutamine, 25 mM HEPES, penicillin and streptomycin 100 international units (IU)/mL (Lonza) and supplemented with 10% fetal bovine serum (FBS, FetalClone II, HyClone, Euroclone). All cells were maintained in a 5% CO2 humidified atmosphere at 37 °C.All cell lines were routinely tested for mycoplasma contamination. Primary human hepatocytes were purchased from Biopredic and cultured following the manufacturer's instructions. Primary human hepatocytes were transduced for 24 h and then cultured for 7 days before gDNA extraction and VCN determination (see "VCN determination"). At this time, primary human hepatocytes transduced with a PGK.GFP LV were analyzed by fluorescence microscopy to determine GFP expression. Nuclei were stained with Hoechst.

RNA extraction and ddPCR

Murine organs, murine primary sorted hepatocytes and LSEC were stored at −80 °C in RLT+ buffer (Qiagen) solution, suggested for RNA extraction. In the case of organs, 300 µl of RLT+ were added to every 25 mg tissue piece. In the case of cells, 250 µl of RLT+ were added by default. Organs were homogenized using gentleMACS™ M Tubes (MACS Miltenyi Biotec, 130096335). Tubes were inserted in gentleMACS™ Octo Dissociator (Miltenyi Biotec) and the protocol selected was gentleMACS program RNA_02, suggested for frozen tissues. Homogenized tissues were subsequently loaded into Maxwell® RSC simplyRNA tissue cartridges and RNA was extracted using simplyRNA tissue method. Cellular RNA was extracted using RNeasy+ mini kit (Qiagen), following the manufacturer's instructions. DNA was digested on columns through RNase-Free DNase Set (Qiagen). Retro transcription was performed using SuperScript IV VILO Master Mix with EzDNase Enzyme (Thermo Fisher), following the manufacturer's instruction. Each sample was retro-transcribed in two wells, one containing the enzyme (RT+), and one without the enzyme (RT−). cDNA was analyzed by ddPCR as described above, using probe systems. RT- signal was subtracted from RT+ signal, resulting in a true signal. For LV-derived *Wpre** custom primers and probe were used. For all the other genes, commercially available primers and probes were used. As normalizer, commercial *Hprt* primers and probe were used. Gene expression levels were calculated with the formula ng cDNA gene/ng cDNA normalizer.

Custom primers and probe, designed and used, were the following:

- *Wpre** Fw: 5′- GGCTGTTGGGCACTGACAAT -3′
- *Wpre** Rv: 5′- ACGTCCCGCGCAGAATC -3′
- HIV Pr 5′-(FAM)- TTTCCATGGCTGCTCGCCTGTGT -(MGB)-3′

Commercial Biorad gene expression assays used were the following:

Ldlr Mus Musculus, dMmuCPE5122114, FAM
Vldlr Mus Musculus, dMmuCPE5114942, FAM
Lrp2 Mus musculus, dMmuCPE5121668, FAM
Lrp4 Mus Musculus, dMmuCPE5195296, FAM
Lrp5 Mus Musculus, dMmuCPE5119884, FAM
Lrp6 Mus Musculus, dMmuCPE5098188, FAM
Sorl1 Mus Musculus, dMmuCPE5103740, FAM
Lrp1 Mus Musculus, dMmuCPE5113466, FAM
Hprt Mus Musculus, dMmuCPE5095493, VIC

Acetaminophen preparation and selection protocol

Acetaminophen (paracetamol; Sigma-Aldrich), was dissolved in saline at 13 mg/mL, filtered 0.22 µm, and stored at room temperature for up to 1.5 months, or until precipitates formation was observed. The selection protocol was performed as previously described[11]. Mice were fasted overnight (for around 16 h) before each acetaminophen administration. On the morning of each injection, mice were weighed, and acetaminophen was given twice or once weekly. The starting dose of acetaminophen was 225 mg/kg in males and 250 mg/kg in females. ALT measurements of ongoing damage were made on bleedings performed 6–7 h after acetaminophen injection. In case of ALT levels under 300 IU/L, the next dose was increased by 5–10 mg/kg. Once ALT levels >300 IU/L, the dose was generally kept for the rest of the experiment. For most experiments, acetaminophen doses were then kept constant. After fasting, if >15% of body weight was lost, acetaminophen treatment was skipped.

ALT, AST, ALP measurements

ALT (#0018257440), AST (#001825740) and ALP (#0018259740) were used for the quantitative determination of the serum with an International Federation of Clinical Chemistry and Laboratory Medicine–optimized kinetic ultraviolet (UV) method in an ILab650 chemical analyzer (Instrumentation Laboratory). SeraChem Control Level 1 and Level 2 (#0018162412 and #0018162512) were analyzed as quality control.

Fractionation and sorting of liver cell sub-populations

The mouse liver was perfused (15 mL/min) via the inferior vena cava with 12.5 mL of the following solutions at subsequent steps: (1) PBS EDTA (0.5 mM), (2) HBSS (Hank's balanced salt solution, Gibco) and HEPES (10 mM), (3) HBSS-HEPES 0.03% Collagenase IV (Sigma). The digested mouse liver tissue was harvested, passed through a 100 µm cell strainer (BD Biosciences) and processed into a single-cell suspension. This suspension was subsequently centrifuged three times (30, 25 and 20 *g*, for 3 min, at room temperature) to obtain hepatocytes-containing pellets. Hepatocytes-containing pellets were stained by diluting in 200 µl of PBS the following antibodies (Table 1).

After 20 min of incubation at room temperature, we washed them with HBSS (Hank's balanced salt solution, Gibco) 1% HEPES (4-(2-hydroxyethyl)-1-piperazineethanesulfonic acid). The nPC contaminating the PC suspension, were removed by FACS excluding cells labeled by APC-conjugated anti-CD31/anti-CD45 cocktail, thus obtaining sorted hepatocytes (Hep) using BD FACSMelody™ Cell Sorter (BD Biosciences) or MoFlo Astrios EQ Cell Sorter (Beckman Coulter). The non-parenchymal cells (nPC)-containing supernatant was centrifuged (650 *g*, 7 min, at room temperature) and recovered cells were loaded onto a 30/60% Percoll (Sigma) gradient (1,800 *g*, for 15 min at room temperature). nPC interface was collected and washed twice. The nPC were subsequently incubated with the following monoclonal antibodies, diluted in 200 µl of PBS (Table 2).

After 20 min of incubation at 4 °C, we washed them with HBSS 1% HEPES. We sorted KC, LSEC, HSC, using BD FACSAria Fusion (BD

Table 1 | List of antibodies for hepatocytes purification by FACS

Antigen	Fluorochrome	Clone	Company (code)	Volume
CD31	APC	MEC 13.3	BD Biosciences (551262)	3 µl
CD45	APC	30-F11	BD Biosciences (559864)	3 µl
FC Block		2.4G2	BD Biosciences (553142)	5 µl

Table 2 | List of antibodies for nPC purification by FACS

Antigen	Fluorochrome	Clone	Company (code)	Volume
CD31	FITC	MEC 13.3	BD Biosciences (551262)	7 µl
CD45	BV786	104	BD Biosciences (563686)	7 µl
F4/80	PE	CI:A3-1	BD Biosciences (553142)	7 µl
CD45R/B220	PE-Cy5	RA3-6B2	BD Biosciences (553091)	7 µl
CD11c	PE-Cy7	N418	Invitrogen (25-0114-82)	7 µl

Biosciences), according to surface marker expression (gating strategy shown in Supplementary Fig. 1c, d).

Liver histopathology analysis

Livers were stored in formalin. Samples were then processed as previously described[5]. Briefly, livers were trimmed, embedded in paraffin wax, sectioned, mounted on glass slides and stained with hematoxylin and eosin (H&E) and Picrosirius red for histopathological evaluation and analysis of collagen deposition. Fibrosis scores were defined as follows: (i) grade 0 if no abnormalities were detected, (ii) grade 1 in case of presence of minimal deposition of collagen central with short septa, focal, (iii) grade 2 in case of presence of mild deposition of collagen central with longer incomplete septa, focal or multifocal. For quantification of glutamine synthetase, staining of slides and acquisition were performed by Centro di Imaging Sperimentale facility in San Raffaele Hospital. Briefly, formalin-fixed paraffin-embedded consecutive sections were dewaxed and hydrated through graded decrease alcohol series and stained for immunohistochemical characterization (IHC). Slides were immunostained with Automatic Leica BOND RX system (Leica Microsystems GmbH, Wetzlar, Germany). First, tissues were deparaffinized and pre-treated with Epitope Retrieval Solution (ER1 Citrate Buffer). Anti glutamine synthetize primary antibody (NB110-41404, Novus Biologicals), diluted 1:1500, was incubated at room temperature and was developed with Bond Polymer Refine Detection (Leica, DS9800). Slides were acquired with Aperio AT2 digital scanner at a magnification of 20X (Leica Biosystems) and analyzed with Imagescope (Leica Biosystem).

Immunohistochemistry with anti Ki67 (SP6 Thermo Scientific, rabbit monoclonal 1:100 Tris-EDTA pH9, 30 min 90°) was performed to evaluate the rate of proliferation of hepatocytes, which was assessed through a semiquantitative analysis. For each mouse, 10 high power fields, 400x magnification, were randomly evaluated on sections of liver. The mean of Ki67 positive hepatocytes for each mouse, followed by the mean of pooled ki67 positive hepatocytes per group were calculated.

Immunofluorescence imaging

Livers were harvested from mice, washed briefly in PBS and fixed 4 h in PBS 4% paraformaldehyde (PFA), then washed again briefly in PBS before being stored at least 24 h in 30% sucrose 0.02% sodium azide in H_2O. Livers were then frozen in OCT (optimal cutting temperature) compound (Killik, Bio Optica) and slices 5–20 µm thick were cut at cryostat (Histo-line MC5050), placed on Superfrost® Plus microscope slides (Thermo Scientific) and stored at −80 °C. All the staining steps were performed protected from lights to preserve endogenous fluorescence. Slides were thawed at room temperature for at least 2 h, then washed 3 times 5 min in PBS 0.1% X-Triton. Edges were drawn around the tissue using immunostaining pap pen (Sigma-Aldrich) to contain staining solutions. The blocking step was performed using PBS 0.1% X-Triton 1% bovine serum albumin (BSA) 5% FBS for 1 h at room temperature in a humid chamber. The blocking solution was then substitute with mix containing primary antibodies in the blocking solution and incubation was carried on for 12–16 h at 4 °C in a humid chamber. The primary antibodies mix solution was removed and slides were washed 3 times 5 min in PBS 0.1% X-Triton. Secondary antibodies were diluted in the blocking solution together with Hoechst (Invitrogen, 1:20,000) and incubated for 1 h at room temperature in a humid chamber. Slides were then washed in PBS and a coverslip was added using Fluoromount-G (Invitrogen) as mounting medium. Slides were dried for 16 h at room temperature or for longer at 4 °C, and stored at 4 °C before acquisition. The following antibodies were used for immunofluorescence staining:

Anti-GFP rabbit, polyclonal (Invitrogen, A11122, 1:1000)

Anti-GFP chicken, polyclonal (Abcam, ab13970, 1:200)

Anti-Rabbit IgG Alexa Fluor (AF)647 donkey, polyclonal (Invitrogen, 1:1000)

Anti-Chicken IgY Alexa Fluor (AF)488 goat, polyclonal (Invitrogen, 1:1000)

Images were acquired using confocal microscope Leica TCS SP5, Leica TCS SP8, or Mavig Rs-G4 at 20X or 40X magnification. Images were analyzed using Image J or MATLAB software. A custom-written Matlab pipeline was used to analyze the images. Briefly, for all the channels (GFP positive and nuclei) we extract black and white masks of the cells/nuclei by background subtraction and applying a fixed threshold. A mask of the tissue is obtained similarly on the image calculated as max projection across all the channels, as previously described[35].

Integration site analysis

Integration sites were retrieved by Sonication Linker Mediated (SLiM)-PCR as previously described[36] with minor modifications. Briefly, each sample was processed in technical triplicates using 100 ng of gDNA. DNA shearing was performed using the Covaris E220 Ultrasonicator, generating fragments with an average size of 1000 bp. The fragmented DNA was subjected to end repair and 3′ adenylation and then ligated to linker cassettes containing a 8 nucleotide sequence barcode used for sample identification, and all the sequences required for the Read 2 paired end sequencing. The ligation products were split into three technical replicates and subjected to 35 cycles of exponential PCR using primers specific for the lentiviral vector LTR and the Linker cassette. A subsequent amplified with additional 10 PCR cycles was performed using a primer specific for the linker cassette and the LTR. These primers contain an 8 nucleotide barcode used for sample identification (coupled with the barcode on the linker cassette) and the sequences needed for the Read 1 sequencing, with additional 12-random-nucleotides allowing easier cluster recognition in the first sequencing cycles in the Next Generation Sequencing (NGS). The generated SLiM-PCR products are thus associated to a unique pair of barcodes, assembled into libraries, and subjected to NGS Illumina sequencing.

Bioinformatics analysis

Sequencing reads were processed using a custom bioinformatics pipeline (VISPA2)[37] that isolates genomic sequences flanking the vector LTR and maps them to the murine genome (mm9). Because vector integration in the same genomic position in different cells is a very low probability event, identical IS in independent samples were considered as contamination or amplification artifacts, which may occur during the technical procedure. Datasets were pruned from potential contaminations and false positives between each primary mouse and from IS deriving from unrelated secondary mice. The identical IS shared between mice belonging to different experimental groups were reassigned based on identification of the insertion site by at least two SLiM technical replicates and sequence count numbers. Downstream analyses of vector IS, such as relative abundance analysis, sharing analysis and IS clustering, were performed using ISAnalytics[38]. Clonal abundance estimates as the relative percentage of genome numbers were determined by the R package "sonicLength"[39]. Regarding IS clustering, we applied Grubbs' test for outliers to determine whether a particular IS exhibits an unusually

high (or low) frequency compared to the overall dataset. The targeting frequency of each gene was normalized for each gene length and transformed into a z-score. This value is compared to the z-score values of the overall dataset by a *t*-student distribution (*p*-values < 0.05)[40]. Regarding cancer genes, we searched for oncogenes and tumor suppressors based on the UniProt database and identified 228 genes classified as proto-oncogenes and tumor suppressors among all targeted genes by LV IS.

FVIII assays

The concentration of human FVIII was determined in mouse plasma by an enzyme-linked immunosorbent assay (ELISA) specific for human FVIII antigen. Microtiter plates were coated with anti-hFVIII binding Ab (Green Mountain Antibodies #GMA8016, 0.2 μg/well in 0.1 M carbonate buffer, pH 9.6) overnight at 4 °C and then blocked for 1 h at room temperature with blocking buffer (PBS 0.05% Tween-20, 1 M NaCl, 10% heat-inactivated horse serum, Gibco). Plasma samples are diluted as needed starting from 1:10 in blocking buffer, added to wells (100 μL/well) and incubated for 2 h at 37 °C. hFVIII was detected by adding detection Ab (Affinity Biologicals, F8C-EIC-D) for 1 h at 37 °C, followed by 5–10 min incubation with 100 μL/well of TMB substrate (Surmodics). Reaction was blocked with HCl 1 N (50 μL/well) and absorbance of each sample was determined spectrophotometrically at 450 nm, using a Multiskan GO microplate reader (Thermo Fisher Scientific) and normalized to antigen standard curve (ReFACTO, Pfizer, from 25 ng/mL – 0.39 ng/mL serially diluted 1:2 in blocking buffer; dilution was corrected with 10% HemoA murine plasma). hFVIII activity in mouse plasma was measured using Coatest SP FVIII (Chromogenix) following the manufacturer's instructions.

FIX assays

The concentration of human FIX was determined in mouse plasma by Affinity's Factor IX Paired Antibody Set (Affinity Biologicals FIX-EIA) consists of matched capture and detecting antibodies that have been titrated and optimized for use in sandwich style ELISA assays following the manufacturer's instructions. Absorbance of each sample was determined spectrophotometrically, using a Multiskan GO microplate reader (Thermo Fisher Scientific) and normalized to antigen standard curves. FIX activity was determined in an activated partial thromboplastin time (aPTT) assay employing Actin-FSL (Siemens) and human FIX-deficient plasma (Diagnostica Stago) and using a semi-automated coagulometer (BioMerieux). Plasma samples were tested at a 1:40 dilution and calibration curves were constructed with serial dilutions of pooled normal human plasma collected from 80 healthy volunteers and arbitrarily assigned a value of 100% FIX activity.

Pcsk9 ELISA

Pcsk9 ELISA was used to assess Pcsk9 concentration in mouse serum samples (R&D Systems, MPC900), following the manufacturer's protocol. The absorbance of each sample was determined spectrophotometrically, using a Multiskan GO microplate reader (Thermo Fisher Scientific) and normalized to antigen standard curves.

Statistics and reproducibility

The sample size in experiments with mice was chosen according to previous experience with experimental models and assays. No sample or animal was excluded from the analysis. Mice were randomly assigned to each experimental group. Investigators were not blinded. Data were presented as individual values with mean ± standard error of the mean (SEM) or as individual values with mean. Statistical analyses were performed upon consulting with professional statisticians at the San Raffaele University Center for Statistics in the Biomedical Sciences (CUSSB). When normality assumptions were not met, non-parametric statistical tests were performed. Two-tailed Mann-Whitney test was performed to compare two independent groups. In the presence of more than two independent groups, the Kruskal-Wallis test followed by post-hoc analysis (Dunn's test for multiple comparisons against the reference control group along with Bonferroni's correction) was applied. Statistical analysis were performed using GraphPad Prism software (10.2.0.392). To model the dynamics of transgene amounts over time, Linear-Mixed Effects (LME) models were estimated, specifying random-effect terms on mouse ID to account for repeated measures data. Whenever needed, to fulfill underlying model assumptions, the outcome variable was transformed using logarithmic or ordered quantile normalization. Following the estimation of LME models, post-hoc analysis was conducted allowing for pairwise comparison of treatment groups at the last time point. To account for the multiplicity issue, *p*-values were adjusted using Bonferroni's approach. LME models were estimated using R software (version 4.3.1). In all the analyses, the significance threshold was set at 0.05. Inferential techniques were applied in the presence of adequate sample sizes ($n \geq 5$), otherwise, only descriptive statistics are reported.

Reporting summary

Further information on research design is available in the Nature Portfolio Reporting Summary linked to this article.

Data availability

The authors declare that the main data supporting the findings of this study are available within the article and its Supplementary Information files. Source data are provided with this paper. The LV and reagents described in this manuscript are available to interested scientists upon signing an MTA with standard provisions. There are some restrictions on the use of the provided materials in research involving LV-based gene therapy of hemophilia, except for research aimed at reproducing the findings reported in this manuscript, according to the collaboration agreement between Fondazione Telethon, San Raffaele Scientific Institute, and GeneSpire. All data associated with this study are available in the main text or the "Supplementary materials". Source data are provided with this paper.

References

1. Zabaleta, N., Unzu, C., Weber, N. D. & Gonzalez-Aseguinolaza, G. Gene therapy for liver diseases - progress and challenges. *Nat. Rev. Gastroenterol. Hepatol.* **20**, 288–305 (2023).
2. Mahlangu, J. et al. Two-year outcomes of valoctocogene roxaparvovec therapy for hemophilia A. *N. Engl. J. Med* **388**, 694–705 (2023).
3. Pipe, S. W. et al. Gene therapy with etranacogene dezaparvovec for hemophilia B. *N. Engl. J. Med* **388**, 706–718 (2023).
4. Ronzitti, G., Gross, D. A. & Mingozzi, F. Human immune responses to adeno-associated virus (AAV) vectors. *Front Immunol.* **11**, 670 (2020).
5. Cantore, A. et al. Liver-directed lentiviral gene therapy in a dog model of hemophilia B. *Sci. Transl. Med* **7**, 277ra228 (2015).
6. Clar, J. et al. Hepatic lentiviral gene transfer prevents the long-term onset of hepatic tumours of glycogen storage disease type 1a in mice. *Hum. Mol. Genet* **24**, 2287–2296 (2015).
7. Milani, M. et al. Phagocytosis-shielded lentiviral vectors improve liver gene therapy in nonhuman primates. *Sci. Transl. Med.* **11**, eaav7325 (2019).
8. Milani, M. et al. Liver-directed lentiviral gene therapy corrects hemophilia A mice and achieves normal-range factor VIII activity in non-human primates. *Nat. Commun.* **13**, 2454 (2022).
9. Nicolas, C. T. et al. In vivo lentiviral vector gene therapy to cure hereditary tyrosinemia type 1 and prevent development of precancerous and cancerous lesions. *Nat. Commun.* **13**, 5012 (2022).

10. Kapelanski-Lamoureux, A. et al. Ectopic clotting factor VIII expression and misfolding in hepatocytes as a cause for hepatocellular carcinoma. *Mol. Ther.* **30**, 3542–3551 (2022).
11. Vonada, A. et al. Therapeutic liver repopulation by transient acetaminophen selection of gene-modified hepatocytes. *Sci. Transl. Med.* **13**, eabg3047 (2021).
12. Vonada, A. et al. Complete correction of murine phenylketonuria by selection-enhanced hepatocyte transplantation. *Hepatology* **79**, 1088–1097 (2024).
13. Yoon, E., Babar, A., Choudhary, M., Kutner, M. & Pyrsopoulos, N. Acetaminophen-induced hepatotoxicity: a comprehensive update. *J. Clin. Transl. Hepatol.* **4**, 131–142 (2016).
14. Santoni de Sio, F. R., Cascio, P., Zingale, A., Gasparini, M. & Naldini, L. Proteasome activity restricts lentiviral gene transfer into hematopoietic stem cells and is down-regulated by cytokines that enhance transduction. *Blood* **107**, 4257–4265 (2006).
15. Brown, B. D. et al. In vivo administration of lentiviral vectors triggers a type I interferon response that restricts hepatocyte gene transfer and promotes vector clearance. *Blood* **109**, 2797–2805 (2007).
16. Hosel, M. et al. Autophagy determines efficiency of liver-directed gene therapy with adeno-associated viral vectors. *Hepatology* **66**, 252–265 (2017).
17. Brown, B. D. et al. A microRNA-regulated lentiviral vector mediates stable correction of hemophilia B mice. *Blood* **110**, 4144–4152 (2007).
18. Mlynarczuk-Bialy, I. et al. Biodistribution and efficacy studies of the proteasome inhibitor BSc2118 in a mouse melanoma model. *Transl. Oncol.* **7**, 570–579 (2014).
19. Bril, W. S. et al. Tolerance to factor VIII in a transgenic mouse expressing human factor VIII cDNA carrying an Arg(593) to Cys substitution. *Thromb. Haemost.* **95**, 341–347 (2006).
20. Kim, Y. et al. A case of drug-induced hepatitis due to bortezomib in multiple myeloma. *Immune Netw.* **12**, 126–128 (2012).
21. Agudo, J. et al. A TLR and non-TLR mediated innate response to lentiviruses restricts hepatocyte entry and can be ameliorated by pharmacological blockade. *Mol. Ther.* **20**, 2257–2267 (2012).
22. Finkelshtein, D., Werman, A., Novick, D., Barak, S. & Rubinstein, M. LDL receptor and its family members serve as the cellular receptors for vesicular stomatitis virus. *Proc. Natl. Acad. Sci. USA* **110**, 7306–7311 (2013).
23. Nikolic, J. et al. Structural basis for the recognition of LDL-receptor family members by VSV glycoprotein. *Nat. Commun.* **9**, 1029 (2018).
24. Takenaka, K. et al. Polymorphism in Sirpa modulates engraftment of human hematopoietic stem cells. *Nat. Immunol.* **8**, 1313–1323 (2007).
25. Milani, M. et al. GP64-pseudotyped lentiviral vectors target liver endothelial cells and correct hemophilia A mice. *EMBO Mol. Med.* **16**, 1427–1450 (2024).
26. Hirai, M. et al. Bortezomib suppresses function and survival of plasmacytoid dendritic cells by targeting intracellular trafficking of Toll-like receptors and endoplasmic reticulum homeostasis. *Blood* **117**, 500–509 (2011).
27. Raedler, L. Velcade (bortezomib) receives 2 new FDA indications: for retreatment of patients with multiple myeloma and for first-line treatment of patients with mantle-cell lymphoma. *Am. Health Drug Benefits* **8**, 135–140 (2015).
28. Loncharich, M. F. & Anderson, C. W. Interferon inhibition for lupus with anifrolumab: critical appraisal of the evidence leading to FDA approval. *ACR Open Rheumatol.* **4**, 486–491 (2022).
29. Browning, J. D. & Horton, J. D. Fasting reduces plasma proprotein convertase, subtilisin/kexin type 9 and cholesterol biosynthesis in humans. *J. Lipid Res.* **51**, 3359–3363 (2010).
30. Morand, E. F. et al. Trial of anifrolumab in active systemic lupus erythematosus. *N. Engl. J. Med* **382**, 211–221 (2020).
31. Aleksunes, L. M., Campion, S. N., Goedken, M. J. & Manautou, J. E. Acquired resistance to acetaminophen hepatotoxicity is associated with induction of multidrug resistance-associated protein 4 (Mrp4) in proliferating hepatocytes. *Toxicol. Sci.* **104**, 261–273 (2008).
32. Shayiq, R. M. et al. Repeat exposure to incremental doses of acetaminophen provides protection against acetaminophen-induced lethality in mice: an explanation for high acetaminophen dosage in humans without hepatic injury. *Hepatology* **29**, 451–463 (1999).
33. Annoni, A., Gregori, S., Naldini, L. & Cantore, A. Modulation of immune responses in lentiviral vector-mediated gene transfer. *Cell Immunol.* **342**, 103802 (2019).
34. Matrai, J. et al. Hepatocyte-targeted expression by integrase-defective lentiviral vectors induces antigen-specific tolerance in mice with low genotoxic risk. *Hepatology* **53**, 1696–1707 (2011).
35. Simoni, C. et al. Liver fibrosis negatively impacts in vivo gene transfer to murine hepatocytes. *Nat. Commun.* **16**, 2119 (2025).
36. Cesana, D. et al. Retrieval of vector integration sites from cell-free DNA. *Nat. Med.* **27**, 1458–1470 (2021).
37. Spinozzi, G. et al. VISPA2: a scalable pipeline for high-throughput identification and annotation of vector integration sites. *BMC Bioinforma.* **18**, 520 (2017).
38. Pais, G. et al. ISAnalytics enables longitudinal and high-throughput clonal tracking studies in hematopoietic stem cell gene therapy applications. *Brief Bioinform.* **24**, bbac5511 (2023).
39. Berry, C. C. et al. Estimating abundances of retroviral insertion sites from DNA fragment length data. *Bioinformatics* **28**, 755–762 (2012).
40. Biffi, A. et al. Lentiviral vector common integration sites in preclinical models and a clinical trial reflect a benign integration bias and not oncogenic selection. *Blood* **117**, 5332–5339 (2011).
41. Franchini, M., Favaloro, E. J. & Lippi, G. Mild hemophilia A. *J. Thromb. Haemost.* **8**, 421–432 (2010).

Acknowledgements

This work was supported by Fondazione Telethon SR-Tiget Core Grant TTACC0422TT to A.C. and the Bioverativ/Sanofi sponsored research agreement. We thank the Advanced Light and Electron Microscopy Bioimaging Center (ALEMBIC, San Raffaele Scientific Institute) for imaging techniques and analysis. We would like to thank Sara Degl'Innocenti for the help with histopathological evaluations, Micol Ravà for liver enzymes assessment, and Luca Basso Ricci for the help with FACS experiments. We thank all the members of the Cantore laboratory for helpful discussions. C.C. conducted this study as a partial fulfillment of his International Ph.D. Course in Molecular Medicine at San Raffaele University, Milan.

Author contributions

C.C. designed and performed experiments, analyzed and interpreted data, and wrote the manuscript. M.M., C.S., F.St. performed experiments, analyzed data, and edited the manuscript. M.V. performed LV integration site analysis. A.F., M.B., and F.R. provided technical support. M.R., R.N. provided technical support related to histopathology analysis. C.B. and F.C. performed statistical analyses. E.M. supervised M.V.'s work. F.Sa. performed histopathology analysis and edited the manuscript. M.G. provided crucial reagents, and intellectual input and edited the manuscript. A.C. supervised and coordinated research, interpreted data, and wrote the manuscript.

Competing interests

C.C. and A.C. are inventors on patent applications submitted by Fondazione Telethon, San Raffaele Scientific Institute, on LV technology related to the work presented in this manuscript. Fondazione Telethon and San Raffaele Scientific Institute, through SR-Tiget, have established a research collaboration on liver-directed LV gene therapy of hemophilia with GeneSpire. The remaining authors declare no competing interests.

Additional information

Supplementary information The online version contains supplementary material available at https://doi.org/10.1038/s41467-025-60073-0.

Correspondence and requests for materials should be addressed to Alessio Cantore.

Peer review information *Nature Communications* thanks the anonymous reviewer(s) for their contribution to the peer review of this work. A peer review file is available.